
A MULTI-MODAL EXPLAINABILITY APPROACH FOR HUMAN-AWARE ROBOTS IN MULTI-PARTY CONVERSATION

ACCEPTED IN "COMPUTER VISION AND IMAGE UNDERSTANDING" JOURNAL ON JANUARY 23, 2025

 **Iveta Bečková***

Faculty of Mathematics, Physics and Informatics
Comenius University Bratislava
Bratislava, 842 48, Slovak Republic
iveta.beckova@fmph.uniba.sk

 **Štefan Pócoš***

Faculty of Mathematics, Physics and Informatics
Comenius University Bratislava
Bratislava, 842 48, Slovak Republic
stefan.pocos@fmph.uniba.sk

 **Giulia Belgiovine**

CONTACT Unit
Italian Institute of Technology
Genova, 16152, Italy
giulia.belgiovine@iit.it

 **Marco Matarese**

CONTACT Unit
Italian Institute of Technology
Genova, 16152, Italy
marco.matarese@iit.it

 **Omar Eldardeer**

CONTACT Unit
Italian Institute of Technology
Genova, 16152, Italy
omar.eldardeer@iit.it

 **Alessandra Sciutti**

CONTACT Unit
Italian Institute of Technology
Genova, 16152, Italy
alessandra.sciutti@iit.it

 **Carlo Mazzola**

CONTACT Unit
Italian Institute of Technology
Genova, 16152, Italy
carlo.mazzola@iit.it

February 3, 2025

ABSTRACT

The addressee estimation (understanding to whom somebody is talking) is a fundamental task for human activity recognition in multi-party conversation scenarios. Specifically, in the field of human-robot interaction, it becomes even more crucial to enable social robots to participate in such interactive contexts. However, it is usually implemented as a binary classification task, restricting the robot's capability to estimate whether it was addressed or not, which limits its interactive skills. For a social robot to gain the trust of humans, it is also important to manifest a certain level of transparency and explainability. Explainable artificial intelligence thus plays a significant role in the current machine learning applications and models, to provide explanations for their decisions besides excellent performance. In our work, we a) present an addressee estimation model with improved performance in comparison with the previous state-of-the-art; b) further modify this model to include inherently explainable attention-based segments; c) implement the explainable addressee estimation as part of a modular cognitive architecture for multi-party conversation in an iCub robot; d) validate the real-time performance of the explainable model in multi-party human-robot interaction; e) propose several ways to incorporate explainability and transparency in the aforementioned architecture; and f) perform an online user study to analyze the effect of various explanations on how human participants perceive the robot.

Keywords Human Activity Recognition · Explainable AI · Transparency · Attention · Human-Robot Interaction · Addressee Estimation

*These authors contributed equally to this work

1 Introduction

The endeavor to decode human intentions and behavior with advanced computer vision techniques is central to the challenge of developing human-aware technologies that can truly understand and support humans in various everyday scenarios. This is particularly evident in robotics, where the development of embodied agents capable of autonomous and meaningful interaction with humans is facilitated by human activity recognition algorithms, granting them a level of human awareness. In humans, the recognition of intentions related to social interaction is not limited to high-level reasoning abilities but anchors its roots in the visual system (McMahon and Isik, 2023). It follows that visual information is crucial to processing and properly understanding social dynamics, and computer vision models represent an integral component of robots’ socio-cognitive abilities.

As the hallmark of human-centered technology, the development of interactive robots is increasingly focused on fostering human trust in artificial systems. Therefore, the accuracy and robustness of the performances are essential but not the only indicators of the system’s reliability. Explainability and transparency are two other critical aspects of designing and evaluating reliable interactive robots (Wortham et al., 2016). Both allude to the understandability of the system: transparency predominantly refers to the visibility of underlying processes leading to a reduction of ambiguity regarding a behavior (Selkowitz et al., 2017), whereas explainability is related to the capability of a system to exhibit the reasons behind its outputs, decisions or behaviors (Ciatto et al., 2020; Miller, 2019). These two qualities are desirable from a dual perspective. In the eyes of developers, who need deep comprehension of the robot to design and assess its functioning, and from the point of view of users, who should be able to intuitively interact with the artificial system (Sciutti et al., 2018).

In the context of Human-Robot Interaction (HRI), communication is a specific type of interaction. Following Jakobson (1981), communication involves the exchange of messages between an addresser (who sends the message) and an addressee (who is entailed to receive it). In the case of spoken messages, the communication is verbal but usually comprises non-verbal elements such as gaze, gestures, poses, etc., which are grasped via vision and are often necessary to properly contextualize the message and to address it to the correct agent (Skantze, 2021). Even though HRI studies rarely go beyond dyadic interactions, the final goal is often bringing robots to social environments, where they are often required to deal with more than one person and, to achieve this aim, be aware of basic social cues ruling multi-party conversations.

Addressee Estimation (AE), i.e., the ability to understand to whom a speaker is directing their utterance (Skantze, 2021), is a specific case of human activity and intention recognition. The speaker identification and correct conversion of speech into text are necessary but not sufficient elements to engage in multi-party conversations. Thus, AE has become a key factor in HRI. As humans, we deeply exploit non-verbal behavior to indicate whom we are addressing (Auer, 2018; Ishii et al., 2016): an ability that robots could greatly take advantage of to engage in conversations more smoothly. Without it, the understanding of the addressee would exclusively depend on the context of the dialogue or specific keywords (such as the name of the addressee), leading to a loss of fluency in the conversation and an increased likelihood of errors.

Taking into account explainability in the context of human-activity-aware robots requires considering the concept from different perspectives: not only the generation of explanations within the architecture and models controlling the robot’s behavior but also their communication to and reception by users. Hence, this work seeks to bind together such diverse points of view that cannot be examined separately. Starting from this broader approach and with the final aim to endow a social robot with explainable addressee estimation skills for multi-party conversation, we address several key gaps in the field of addressee estimation (AE) for human-robot interaction (HRI). First, we introduce the concept of explainability into AE, leveraging attention-based mechanisms, which, to our knowledge, have not been previously explored in this context. Second, we tackle the limitations of existing AE approaches, which typically only determine if the robot is being addressed, by enhancing the system to identify specific addressees in multi-party conversations. Building on the work of Mazzola et al. (2023), we optimize their addressee direction estimation model and integrate it into a modular architecture for multi-party interaction, incorporating additional components to enable the robot not only to understand basic communication dynamics but also to leverage communication cues and infer the presence of new people in the environment. Finally, while explainability has been studied in related areas such as sentiment analysis and emotion recognition, we provide the first real-time explainable solution for robotic behavior in multi-party conversations, offering both enhanced transparency and practical utility for HRI scenarios.

The contribution of this work is divided into two intertwined steps, whose methodology is described in Section 3. Specifically, in Subsection 3.1, we design and train an attention-based neural network to optimize a former AE model (Mazzola et al., 2023) while extracting explanations at different stages of the inference. In Subsection 3.2, we deploy the newly developed explainable model in a modular robotic architecture to enable the iCub robot to engage in multi-party

conversation, implement a multi-modal system to provide real-time explanations of its behavior, and explore the users' reception of different modalities of explanation (verbal, embodied, graphical) in a user study.

2 Related work

2.1 Attention-based and explainable neural networks

Explainable models are becoming increasingly important in machine learning (Barredo Arrieta et al., 2020). Early efforts focused on using simple models to ensure inherent interpretability. However, as deep learning models improved and outperformed simpler ones (Krizhevsky et al., 2012), achieving even superhuman performance in some tasks (He et al., 2015), their lack of transparency became a significant concern. This has made explainability essential, particularly for deploying deep models in critical applications.

Two widely researched and popular methods for deep learning interpretability are SHAP (Lundberg and Lee, 2017) and LIME (Ribeiro et al., 2016). These, along with similar approaches, train a simpler surrogate model to approximate the black-box model's outputs, making it inherently more explainable.

Latent representations of inputs are often analyzed to understand model behavior. However, their high dimensionality often makes visualization and explanation challenging. To achieve this, dimensionality-reduction techniques can project the complex data into 1D, 2D, or 3D space, enabling clearer data visualization. Principal Component Analysis (PCA), t-distributed Stochastic Neighbor Embedding (t-SNE), and Uniform Manifold Approximation and Projection (UMAP) are commonly used to reduce the space dimensionality, each having its advantages and disadvantages (van der Maaten and Hinton, 2008; McInnes et al., 2018).

On the other hand, there is often a need to generate precise explanations for the image classification domain. For this, saliency maps, i.e., the importance of image regions for predictions, are often investigated (Simonyan et al., 2014; Zhou et al., 2016; Selvaraju et al., 2017). Using these methods, it is possible to peek inside the black-box model processing an image. A downside of these approaches is their dependence on a specific type of architecture (smooth gradients, convolutions, etc.); otherwise, they are often unable to produce satisfying results.

A branch of research, currently setting the state-of-the-art (SOTA) in the majority of tasks, was initiated by designing the transformer architecture (Vaswani et al., 2017) followed by its adaptation for the image domain (Dosovitskiy et al., 2021). Thanks to their attention mechanism, transformers are also often considered more interpretable (Kashefi et al., 2023), as one can extract the attention weights during the forward pass.

Thus, in this work, we leverage the idea of attention in general (Shen et al., 2017; Niu et al., 2021) and the many ways of implementing it in the specific downstream task of AE where, to our knowledge, explainability was never taken into account before.

2.2 Multi-party conversation in HRI

The management of multi-party conversations requires robots to be endowed with human activity recognition capabilities. Several tasks need to be solved to this aim, not only sound detection and natural language understanding, which are essential to receiving the message. Speaker recognition and diarization, turn-taking, and addressee estimation are crucial problems that need to be tackled to assess beyond the "what" of the message, the "who" and the "to whom" of each utterance (Gu et al., 2022). Endowed with multiple sensors, robots can solve multi-party conversation problems with a multi-modal approach to recognize the scene and human intentions via audio, vision, and interpreting information coming from the conversation context (Bilac et al., 2017; Dhaussy et al., 2023; Bae and Bennett, 2023; Addlesee et al., 2024).

Unlike dyadic scenarios, multi-party conversations introduce the challenge of determining who should take the turn when the speaker yields. For the conversation to continue, correctly identifying the addressee(s) typically indicates the next speaker. Keywords, gaze, pose, para-verbal cues, and contextual information have all proven useful for Addressee Estimation (AE) (Skantze, 2021). AE enhances robots' conversational abilities by informing both *when* to intervene and *how* to do so.

In the majority of cases, works tackling AE during the interaction with artificial agents designed rule-based algorithms (Richter et al., 2016), machine learning models (van Turnhout et al., 2005; Huang et al., 2011; Sheikhi et al., 2013), deep neural networks (Mazzola et al., 2023; Tesema et al., 2023) or large language model (LLM) based techniques (Addlesee et al., 2024), grounded on multiple modalities and features to cope with the ambiguity and unpredictability of human behaviors in real-time interactions. However, most current models predict only whether the robot was addressed in a binary way (van Turnhout et al., 2005; Huang et al., 2011; Sheikhi et al., 2013; Tesema et al., 2023; Addlesee et al.,

2024). This approach is unsuitable for multi-party interactions; therefore, it is insufficient for the robot to effectively engage in conversations with more than two humans without pre-determined knowledge about other users' presence.

To resolve this limitation, Mazzola et al. (2023) adopted a deep-learning approach to estimate the direction of the addressee from the robot's perspective, training the model on HRI data collected with a Nao robot (Jayagopi et al., 2012). The same model was then ported and tested with a pilot experiment on the iCub platform (Mazzola et al., 2024), but not yet implemented in an architecture for multi-party conversation. After optimizing the approach of Mazzola et al. (2023), we implemented the new explainable AE model into a more complex modular architecture to allow the robot to identify the addressee outside its field of view.

2.3 Explainability in HRI

Explainable Artificial Intelligence (XAI) has predominantly been explored in the human-computer interaction field (Lai et al., 2021; Gambino and Liu, 2022) but there are still a few studies about XAI within the HRI context (De Graaf and Malle, 2017). Robots introduce additional layers of complexity to the explainability problem than virtual agents due to their embodiment and the higher number of interaction modalities they can handle (Setchi et al., 2020).

Regarding robot planning, Chakraborti et al. (2017) generated explanations while trying to resolve the discrepancies between the robot and human's internal models. Diversely, Tabrez et al. (2019) tackled the problem by focusing on users' task understanding to detect incomplete or incorrect beliefs about the robot's functioning. Instead, concerning human-robot collaboration, Matarese et al. (2023a) focused on explainable robots' influence when providing explanations that consider their common ground, also regarding people's personality traits (Matarese et al., 2023b).

Visual explanations have also been explored in robotics (Maruyama et al., 2022; Halilovic and Lindner, 2023). Notably, Zhu et al. (2022) introduced a multi-modal framework combining visual and verbal explanations for facial emotion recognition. Additionally, Sobrín-Hidalgo et al. (2024) presented a preliminary study on a vision-language model enabling robots to generate explanations by integrating log and video data.

In recent years, the HRI community has shown a growing interest in verbal explanations, destined to grow further because of the spreading of LLMs. For example, Stange et al. (2022) designed and developed a dialogical model for explanations in HRI, which allows robots to reply to human users' requests and explain their internal state. The authors stressed the iterative nature of their model in managing the explanatory processes as dialogues. Task understanding has also been investigated from a dialogical perspective focusing on the role of negation in human-robot explanatory exchanges (Groß et al., 2023). Moreover, to allow artificial agents to adapt their explanations to their partners' understanding, Robrecht and Kopp (2023) implemented a linguistic explainer model that constructs and employs a partner model.

In the context of multi-party conversation, explainability has been investigated for sentiment analysis of social media dialogues (Sinha et al., 2021) and emotion recognition with multi-modal attentive learning (Arumugam et al., 2022). However, to our knowledge, there is no approach to provide real-time explainable and transparent solutions for robot behavior in multi-party interaction.

3 Methods

3.1 Design of the attention-based explainable AE model

The development of our explainable AE model consists of two steps: in the first step, we focus on enhancing the classification accuracy with respect to the previous SOTA in the same task (Mazzola et al., 2023), which represents our baseline (see Paragraph 3.1.1). This way, we obtain a first model, which we refer to as the Improved Addressee Estimation (IAE) model. In the second step, we modify this model using inherently explainable modules based on attention (see Paragraph 3.1.2) to extract additional information during addressee estimation. We refer to the second model as Explainable Addressee Estimation (XAE) model¹.

3.1.1 Improved Addressee Estimation model

Following Mazzola et al. (2023), we use the Vernissage dataset (Jayagopi et al., 2012, 2013) to train an Improved model for the Addressee Estimation task (IAE model). To the best of our knowledge, the Vernissage dataset is one-of-a-kind and designed specifically for solving the task of addressee classification in human-robot interaction. The dataset contains recordings of multi-party conversations from the robot's point of view. In each conversation, one robot and two

¹The implementation can be found here: <https://github.com/iveta331/Explainable-Addressee-Estimation>

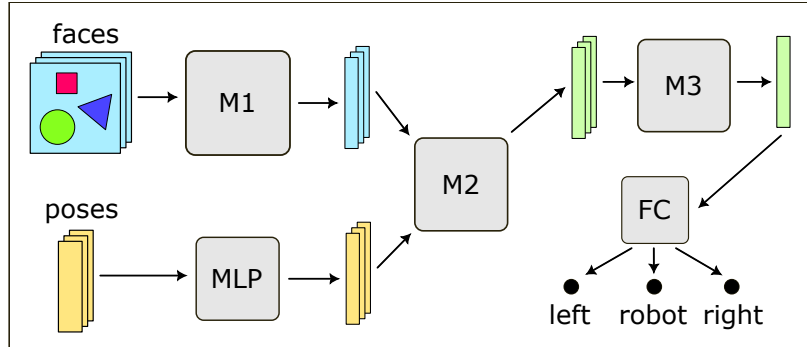


Figure 1: Illustration of the addressee classification workflow. The sequence of faces is embedded using a vision transformer (M1), whereas poses are processed via an MLP. These embeddings are then fused using an intermediate network (M2), and their representation for each time frame is processed by a recurrent network enhanced with attention, forming a unified embedding of the whole utterance. The final step is the mapping to three output options via a fully-connected (FC) layer.

human participants are engaging in a conversation about paintings on the wall. The conversations are manually labeled with the relative position of the addressee from the robot’s point of view. The possible labels are ROBOT, RIGHT, LEFT, GROUP, and NO-LABEL.

To consistently compare with the baseline (Mazzola et al., 2023), we only use the conversation parts in which ROBOT, RIGHT, or LEFT is the target. We also follow the same data pre-processing and data augmentation. To fully leverage the Vernissage dataset, we further augment the input images using commonly recognized techniques. It involves diversifying the lightning conditions (slight changes in brightness, contrast, saturation, and hue), applying spatial changes (rotation and crop), and blurring the images. The exact ranges for each of the data augmentation methods are detailed in Tab. 1. The view from the robot’s camera is split into two parallel data streams (face images and body-pose vectors), which serve as input to the network and later are merged to form a combined representation.

The model from (Mazzola et al., 2023) is further modified by reducing the number of output neurons from the convolutional neural network (CNN) processing the facial information. Also, we replace the convolution on body-pose vectors with fully connected layers. The output dimensionality is chosen to make the length of the outputs from face and pose models similar, allowing for more sophisticated data-fusion methods. Thanks to these modifications, our IAE model improves the current SOTA while significantly reducing the number of trainable parameters ≈ 135 folds (from 91,706,749 to 677,623).

3.1.2 Explainable addressee estimation model

In this section, we describe our neural network architecture (XAE model) that, in addition to yielding accuracy comparable with the IAE model, combines multiple attention-based components, allowing us to extract human-readable explanations.

The information flow in our “explainable” architecture is distinct from our IAE model. First, we utilize a vision transformer instead of a convolutional network to obtain the face representation (Dosovitskiy et al., 2021)². Second, we insert an additional shallow model to fuse the face and pose information. Third, we alter the penultimate processing step using a tailored attention mechanism in the recurrent neural network. This way, we achieve the embedding calculation containing means to provide us with importance scores for each frame. The overall scheme of the addressee estimation is shown in Figure 1.

Most of the above-listed components added to enhance the explainability of the network can be classified as attention mechanisms. A typical approach to incorporating attention into machine learning is to compare similarities of latent representations utilizing the dot product (Niu et al., 2021). The resulting scores can be used for further activation propagation, where, in theory, only the relevant information is further processed. While it is seemingly straightforward, the information flow and the attention computations can be complex enough to fully replace entire layers of deep networks.

²For ViT implementation, we use (Wightman, 2019).

Merging modalities After forming the face embedding ($\mathbf{f}_t \in \mathbb{R}^{d_{\text{face}}}$) using a vision transformer and a pose embedding ($\mathbf{p}_t \in \mathbb{R}^{d_{\text{pose}}}$) using an MLP, we devise a way to combine these representations. The simplest way to achieve this goal is concatenating the two vectors, but it does not admit extracting their relative importance.

Coherently with our goal, i.e., designing an architecture consisting of multiple components with inherent explainability, we seek to know which modality is more important in each time frame. Inspired by Brauwers and Frasinca (2023), we opt for the following variant of a scoring function:

$$\text{score}(\mathbf{v}) = \mathbf{w}_D^T \text{ReLU}(\mathbf{W}\mathbf{v} + \mathbf{b}), \quad (1)$$

where $\mathbf{w}_D \in \mathbb{R}^{d_{\text{inner}}}$, $\mathbf{W} \in \mathbb{R}^{d_{\text{inner}} \times d_v}$, $\mathbf{b} \in \mathbb{R}^{d_{\text{inner}}}$ are trainable parameters, d_{inner} is a hyper-parameter to be optimized, and d_v is the length of the input vector \mathbf{v} . Therefore, in this case, $d_{\text{face}} = d_{\text{pose}} = d_v$.

To compare the influence of each of the two vectors (face and pose) at every frame, we calculate their relative contributions $s_{\mathbf{f}_t}$, $s_{\mathbf{p}_t}$, as:

$$s_{\mathbf{f}_t}, s_{\mathbf{p}_t} = \text{softmax}(\text{score}(\mathbf{f}_t), \text{score}(\mathbf{p}_t)). \quad (2)$$

Finally, the single-vector representation of both modalities is formed by an element-wise addition of \mathbf{f}_t and \mathbf{p}_t , using their corresponding weights:

$$\mathbf{r}_t = s_{\mathbf{f}_t} \mathbf{f}_t + s_{\mathbf{p}_t} \mathbf{p}_t. \quad (3)$$

Recurrent attention To form a single vector representation of the whole utterance ($\mathbf{r}_1, \dots, \mathbf{r}_n$), in the baseline architecture, we employ a recurrent network. However, to create the ‘‘explainable’’ alternative, we go beyond the ordinary recurrent network and add a form of attention mechanism (as suggested in Brauwers and Frasinca (2023)) that allows us to measure the time frame importance scores while producing the output. Our computation is as follows.

Let us denote a stacked representation through all the time frames of the embeddings created in the previous step as $\mathbf{R} = [\mathbf{r}_1, \mathbf{r}_2, \dots, \mathbf{r}_n]$. We linearly project them to produce keys, queries, and values:

$$\mathbf{Q}_r = \mathbf{W}^Q \mathbf{R}, \quad \mathbf{K}_r = \mathbf{W}^K \mathbf{R}, \quad \mathbf{v}_r = \mathbf{W}^V \mathbf{R}. \quad (4)$$

The queries are then fed one by one into the gated recurrent unit (GRU) network (Cho et al., 2014), to eventually form the embedding \mathbf{q} integrating the information about all the time frames. Using the query embedding \mathbf{q} , we proceed to the computation of the similarities with keys encoded in the matrix \mathbf{K} , providing the contribution scores ($\mathbf{c} = \mathbf{K}\mathbf{q}$) of each time frame. To produce the final utterance representation \mathbf{u} , we use element-wise addition on elements of \mathbf{V} , with the weight provided in \mathbf{c} :

$$\mathbf{u} = \sum_{i=1}^n c_i \mathbf{v}_i. \quad (5)$$

A fully-connected layer taking \mathbf{u} as input produces the final addressee estimation. A graphical illustration of our recurrent block is provided in Figure 2.

3.1.3 Generating explanations

The architectural design of the model is proposed with the intention for the explanations to be inherent. That way, one does not need an extra post-processing step to extract explanations, rendering our model computationally efficient and suitable for use in systems where real-time feedback is necessary. Three types of explanations are included: 1) image saliency, 2) face vs. pose importance, and 3) time frame importance.

Image saliency To process an image via the vision transformer, we first need to split the image into small patches — non-overlapping squares forming the entire image. The patches are further embedded and subjected to the attention blocks. Those consist of multiple self-attention layers (multi-head self-attention), residual connections, batch normalization, and fully connected layers, all repeated several times (Vaswani et al., 2017). For visualization purposes, we are primarily interested in the self-attention computation, defined by the formula:

$$\text{Attention}(\mathbf{Q}, \mathbf{K}, \mathbf{V}) = \text{softmax} \left(\frac{\mathbf{Q}\mathbf{K}^T}{\sqrt{d_k}} \right) \mathbf{V}. \quad (6)$$

The matrices \mathbf{Q} , \mathbf{K} , and \mathbf{V} carry the information about each image patch. Thus, visualizing the raw attention scores provided after the softmax computation up-sampled back to the original image size produces maps, highlighting the areas the network uses the most for further processing. A sample depiction of the attention map is provided in Figure 3. Since employing multiple parallel heads in the vision transformer is a common practice, we have more visualization options. Because the attention heads extract different features, combining them for visualization can produce more consistent maps.

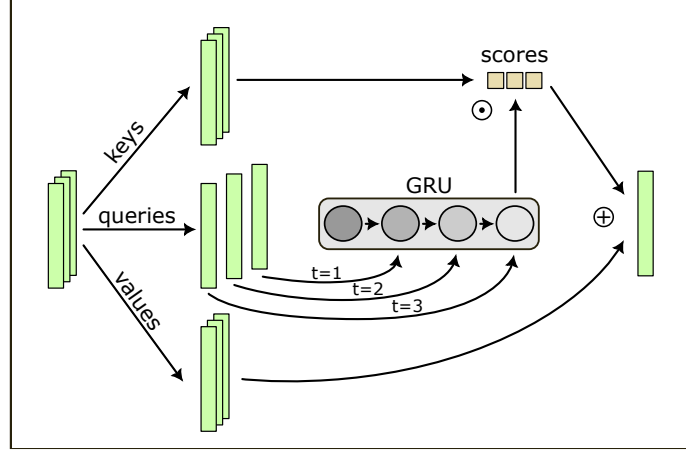


Figure 2: The scheme of the recurrent network augmented with an attention mechanism. The input sequence (left) is projected to form keys, queries, and values. The queries are fed to the GRU network to obtain a single query. That is used to match the keys and compute the scores, which are used to sum up the values (forming the output).

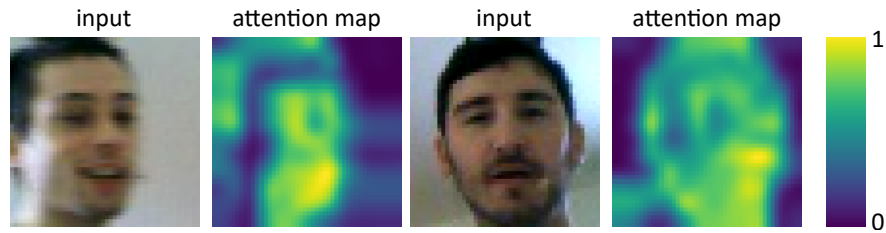


Figure 3: Attention maps extracted from the penultimate layer of the vision transformer employed in the model. The yellow areas indicate active information flow, whereas the blue areas correspond to patches that are not significant at the current layer.

Face vs. pose To see the relative importance of face vs. pose information, we can extract the weights used to combine these modalities. Knowing which modality was used more/less can provide the speaker with clues about what was unclear when misclassifications occurred.

Even though the weight extraction is straightforward, some interesting intrinsic properties exist. The general hyper-parameter setup, as well as the whole architecture, have a huge impact on the expressiveness of the model. For a concise analysis of the weights distribution, see Subsection 4.2.

Time frame score The attention weights provided in the recurrent network offer an ideal way for us to retrieve information about those time frames, which have the highest impact on the classification.

Using attention activations, we design a method to automatically generate a verbal cue about the most important part of the prediction. To capture this, we use the average of the attention weights in a sliding window. The average is compared to a threshold θ , and if it crosses the $\frac{1}{k} + \theta$, where k is the length of the sequence, an output sentence is generated based on the sliding window location. For simplicity, in this experiment, we distinguish between three possibilities of the important region: the beginning of the interaction, the middle, and the end.

Two samples of a response, given sequences of length 10, are shown in Figure 4. We can see the weights of individual time frames distinguished by the color and size of the red dots. Even though these explanations are particularly easy to interpret, the generation process includes the pose information as well, which is for clarity not included in the image.

3.1.4 Training and performance evaluation

To achieve the best possible performance of our models, we perform a hyper-parameter search. We always keep one of the 10 interactions included in the dataset for testing and perform 9-fold cross-validation on the remaining 9 interactions. This cross-validation performance (weighted according to the number of sequences in individual interactions) is being optimized. We use WandB Biewald (2020) with Bayesian search for the optimization.

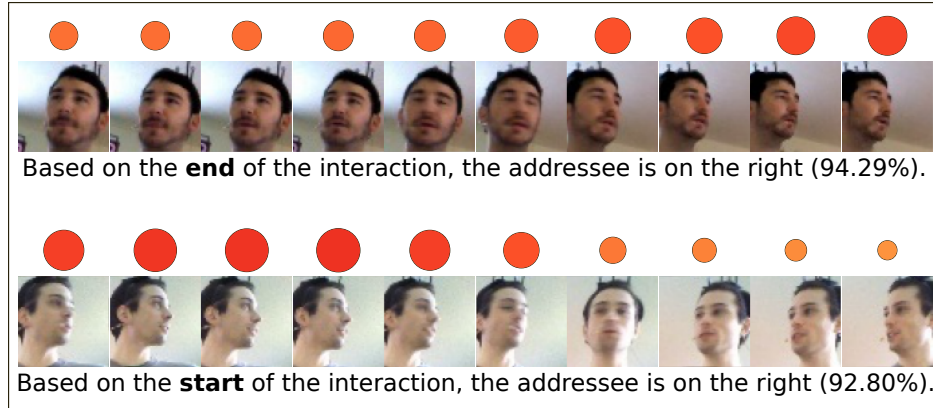


Figure 4: Visualization of two sequences, with their corresponding attention scores (dots) generated by the recurrent network, alongside the generated explanations. The dots’ color and size correspond to the attention score magnitude for each time frame.

After choosing all the hyper-parameters, we train a network on nine conversations and test with the remaining one. This is repeated ten times (for all possibilities of the test set). To calculate the final F1 score, we average the results across classes (weighted by the number of samples in the given class) and then across the 10 trials according to the number of sequences in the test sets.

The most extensive hyper-parameter search was performed for the IAE network, as this was the first one being optimized. Values of some of the less important parameters (e.g. parameters of the data augmentation) were then kept the same for all other networks. The list of all optimized hyper-parameters along with all considered values and the chosen values is provided in Table 1. The hyper-parameters were split into multiple groups, which were being optimized separately. They are ordered and grouped approximately (some parameters were present in multiple groups) in the order in which their value was chosen and fixed. “Gamma” controls the learning rate decay. “Convolutional” controls the number of output channels: “small” = [6, 8, 12, 16], “medium” = [8, 12, 16, 32], “large” = [8, 16, 32, 64]. The last eight hyper-parameters control additional data augmentation. The final IAE model architecture is summarized in Table 2.

The number of hyper-parameters optimized for the XAE model was much lower. They were optimized in two groups. The first group contained optimization-related parameters, such as gammas and learning rates, the second group contained architecture-related parameters. The resulting values are in Tables 3 and 4, while the latter mentioned also contains information about the network architecture. Activation function in the recurrent network is used on inputs to the GRU unit and outputs from the GRU (i.e., inputs to the final fully-connected layer).

Finally, while we utilize the Vernissage dataset for exploring the model’s accuracy and the possibilities for generating explanations, to ensure the resulting model is capable of making correct estimates in an online setting, we also retrain our XAE model on both the Vernissage and a dataset collected using the iCub robot (Saade, 2023). The dataset contains five recorded interactions of three people and the iCub, and is labeled into three groups (LEFT, RIGHT, ROBOT), such that it can be used to extend the Vernissage dataset.

3.2 Implementation of the explainable modular architecture in the robotic platform

After the design, training and testing of the XAE model, the second major contribution of this paper is its deployment in a robotic modular architecture for HRI multi-party conversation, which goes in parallel with an assessment of the two primary features of the architecture: 1) the AE abilities, tested in real-time multi-party interaction, and 2) the explainability and transparency qualities, evaluated through an online user study.

The term artificial cognitive architecture generally refers to computational frameworks that aim to explain and reproduce the fundamental mechanisms of human cognition, such as perception, attention, action selection, memory, learning, reasoning, meta-cognition, or prospective (Vernon, 2014). The development of artificial cognitive architectures able to solve all these tasks with similar performance to humans is a longstanding and unsolved problem (Kotseruba and Tsotsos, 2020). The architecture we propose in this paper is not meant to represent a comprehensive solution for a multi-task robotic architecture. Rather, it is a cognitively-inspired framework supporting the robot’s autonomous reasoning, decision-making, and interaction in the context of a multi-party conversation for deploying and evaluating the proposed explainable model in HRI.

Table 1: List of all considered hyper-parameters for the IAE model and their values ([min, max] range for real-valued ones, set of values for discrete). The last column contains the chosen values.

Parameter name	Considered values	Chosen value
num_epochs	{5, 6, ..., 50}	15
normalisation	{true_stats, imagenet}	true_stats
dropout	{0, 0.1, 0.2, 0.3}	0.2
act1	{ReLU, Tanh}	Tanh
act2	{ReLU, Tanh}	Tanh
act3	{ReLU, Tanh}	Tanh
hid1	{128, 129, ..., 400}	256
hid2	{16, 17, ..., 40}	32
hid3	{16, 17, ..., 40}	32
out1	{10, 11, ..., 64}	32
out2	{10, 11, ..., 32}	20
out3	{8, 9, ..., 32}	20
optimizer1	{SGD, Adam, RMS}	RMS
optimizer2	{SGD, Adam, RMS}	RMS
optimizer3	{SGD, Adam, RMS}	Adam
post_fusion	{LSTM, GRU}	GRU
convolutional	{small, medium, large}	large
gamma1	[0.5, 1]	0.75
gamma2	[0.5, 1]	0.9725
gamma3	[0.3, 1]	0.5
learning_rate1	$[e^{-10}, e^{-7}]$	0.00018
learning_rate2	$[e^{-10}, e^{-2}]$	0.01
learning_rate3	$[e^{-10}, e^{-7}]$	0.00009
batch_size	{10, 11, ..., 350}	16
brightness	[0, 0.5]	0.2
contrast	[0, 0.5]	0.4
saturation	[0, 0.5]	0.45
hue	[0, 0.25]	0.135
angle	[0, 45]	25
crop	[40, 50]	50
kernel_size	{1, 3, 5, 7, 9}	7
sigma	[0.1, 3]	0.8

3.2.1 Deployment of the XAE in a modular architecture

Our architecture³ (Figure 5) is based on the architectural implementation described in Belgiovine et al. (2022). It is based on a *modular* approach where each component (i.e., *a module*) implements a specific robot’s ability (e.g., detecting faces, processing speech, reasoning about the next best action). Such modules exchange information and communicate with each other through the YARP middleware (Metta et al., 2006). To enhance computational resource allocation and optimize time response efficiency, we rely on a distributed approach. This modular setting allows us to incrementally add or update the robot’s skills by integrating additional modules into the framework at later stages.

Audio Perception and Processing Raw audio is given as input to the *Sound Detection* module (Eldardeer et al., 2021). Based on dynamic thresholding to detect speech and a silence buffer threshold of 1.5 seconds to detect the end of an utterance, this module is programmed to trigger every 0.02 second the *Self-Monitoring* module for the utterance segmentation and the consequent activation of the addressee estimation module.

For the Speech-To-Text module, we use the SOTA Whisper⁴ (Radford et al., 2023) “small-distil” model for English language, designed by OpenAI for accurate and robust speech-to-text transcription. Connected in input directly with the microphone and with the speech synthesizer, this module is implemented to synthesize speech while ignoring self-produced utterances.

³Code available at <https://gitlab.iit.it/cognitiveInteraction/explainablemultipartyconversationCVIU.git>

⁴<https://github.com/openai/whisper>

Table 2: Architecture of our final IAE model. All convolution layers use kernel size 5. Relevant layer-specific hyper-parameters are listed in the brackets.

Face image model (net 1)	
Input	50x50 px RGB images
Convolution	8 output channels
Activation (act1)	Hyperbolic tangent
Convolution	16 output channels
Activation (act1)	Hyperbolic tangent
Max-Pool	Kernel of size 2×2
Dropout (dropout)	$p = 0.2$
Convolution	32 output channels
Activation (act1)	Hyperbolic tangent
Convolution	64 output channels
Activation (act1)	Hyperbolic tangent
Max-Pool	Kernel of size 2×2
Dropout (dropout)	$p = 0.2$
Flatten	
Fully-connected (hid1)	256 output neurons
Activation (act1)	Hyperbolic tangent
Fully-connected (out1)	32 output neurons
Pose model (net 2)	
Input	Vector of length 54
Fully-connected (hid2)	32 output neurons
Activation (act2)	Hyperbolic tangent
Fully-connected (out2)	20 output neurons
Recurrent model (net 3)	
Input	Concat. of outputs
GRU block (post_fusion, hid3)	32 hidden neurons
Dropout (dropout)	$p = 0.2$
Fully-connected (out3)	20 output neurons
Activation (act3)	Hyperbolic tangent
Fully-connected	3 output neurons

Table 3: Hyper-parameters of the XAE model. Parameters with indices 1 – 4 control Vit (M1), MLP for pose vectors, intermediate network (M2), and GRU with attention (M3) respectively.

XAE model hyper-parameters	
gamma1	0.70807
gamma2	0.96882
gamma3	0.51241
gamma4	0.9274
learning_rate1	0.00003791
learning_rate2	0.00117708
learning_rate3	0.00185
learning_rate4	0.00006085
optimizer1	RMS
optimizer2	RMS
optimizer3	RMS
optimizer4	Adam
batch_size	4
num_epochs	8

Table 4: Hyper-parameters/architecture of our final XAE model. For processing face images, we use the standard vision transformer architecture, therefore, for brevity, we only provide the chosen hyper-parameter values. The architecture of the recurrent part is discussed in more detail in Paragraph 3.1.2.

Face image model (ViT)	
Input	50x50 px RGB images
Patch size	4x4 px
Embedding dimension	42
Depth	6
Num. heads	6
Output dimension	185
Pose model (fully-connected)	
Input	Vector of length 54
Fully-connected	73 output neurons
Activation	Hyperbolic tangent
Fully-connected	185 output neurons
Intermediate (data-fusion) model	
Input	Two 185-dimensional vectors
Fully-connected	14 output neurons
Activation	ReLU
Fully-connected	1 output neuron
Normalization	Softmax, outputs weights
Weighted sum of inputs	Output vector of length 185
GRU with attention (recurrent) model	
Input	Sequence of 185-dim. vectors
Values dimension	81
Keys dimension	20
GRU hidden dim.	20
Activation	Hyperbolic tangent
Fully-connected	81 inputs, 3 outputs

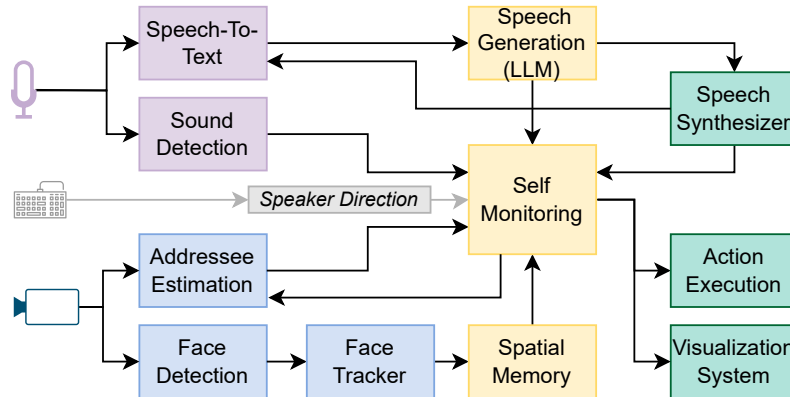


Figure 5: scheme of the modular architecture implemented in the robot iCub. In pink are the audio processing modules, in light blue are visual processing, in yellow are modules to support reasoning processes, and in green are modules to act in the world.

Vision perception and processing Visual input from the robot’s cameras (RGB images of 480x640 resolutions, recorded at 30 fps) is given as input to the *Face Detection* and the *Addressee Estimation* modules to extract higher-level visual features. The *Face Detection* module extracts the bounding boxes of faces using the Ultralytics YOLOv8 model⁵ (Jocher et al., 2023), which has been adapted for working on the iCub YARP-based framework.

The *Addressee Estimation* module deploys our XAE model in the YARP middleware. It pre-processes visual information at 12.5 Hz as in Mazzola et al. (2024), computing the speaker’s body pose using a lightweight version of OpenPose

⁵<https://github.com/ultralytics/ultralytics>

(Cao et al., 2019; Osokin, 2018) and cropping an image of the speaker’s face from the body joints of the head. At each timeframe, the two inputs are given to the XAE model, as described in Section 3.1. After 10 frames, the model returns an estimate of the addressee’s direction relative to the speaker and from a first-person perspective: toward left, right, or directly at the robot. Estimates are sent to the *Self-Monitoring* module. The model takes the frames as input cumulatively until the end of the utterance, triggered by the *Sound-Detection* module via the *Self-Monitoring/State Controller* module, when a final estimate is provided.

A *Multiple Objects Tracker* (MOT) is used to generate tracker instances with a unique ID for each bounding box received by the *Face Detector*. Employing a fusion of the Kalman Filter and Hungarian algorithm, this module ensures consistent identity between faces detected in consecutive frames, allowing real-time performances (Bewley et al., 2016). If necessary, it activates a tracking mode for the robot, enabling it to follow individuals as they move within the environment and update their position when they stop moving (Belgiovine et al., 2022).

Short-Term Spatial Memory A memory system is a core component of a cognitive architecture to facilitate the accomplishment of high and low-level cognitive abilities such as attention, reasoning, and context understanding. Such abilities become particularly crucial in dynamic interactions involving multiple individuals, enabling the robot to maintain awareness of surrounding events despite its attention being focused on limited evidence. When developing artificial cognitive architectures, researchers usually adhere to the traditional classification of memory types established in cognitive psychology (Atkinson and Shiffrin, 1968), attempting to reproduce their basic functionalities and features.

For the purpose of the current work, our *Spatial Memory* module aims to implement the ability of the robot to remember and update the position of elements of interest (in this case, people) in its surrounding environment with respect to an egocentric frame. Hence, the module can be viewed as akin to a short-term spatial working memory system, as the information is solely retained to fulfill the current task, namely attending and intervening appropriately in conversations. No information is stored for subsequent learning or retrieval in future interactions.

This module primarily serves to centralize spatial and contextual knowledge. It aggregates information coming from the MOT and the proprioceptive data derived from the robot’s neck and head encoders (Roncone et al., 2016), linking each tracker instance with the robot’s head orientation and, after a 3-bin discretization, categorizing it as being to the right, left, or in front of the robot. This process creates a dictionary associating each individual with their respective robot-centric spatial position. With a frequency of 2 Hz, each element within this dictionary is dynamically updated with properties pertinent to the multi-party conversation task: people’s role in the interaction (e.g., speaker, listener, addressee). This dictionary structure works as a knowledge repository, formatted in a readable and standardized manner, which remains readily accessible for online queries by any other module that can efficiently update or retrieve information by using any object or property as a key. For example, the module *Self-Monitoring* can ask the *Spatial Memory* for all the items present to the left of the robot or ask for the location of a specific individual.

Speech Generation In order to make the robot able to understand verbal language and give contextual answers, we use an open-weight Large Language Model, specifically the Mistral-7B-Instruct model from MistralAI (Jiang et al., 2023), and deploy it in the architecture as a YARP-based module. Our approach involves simply prompt-engineering specific contextual information to enable the robot to engage meaningfully in multi-party conversations. Details of the prompts used can be found in the Appendix C.

Robot Actions and Behaviors For tracking faces and directing the robot’s head towards the identified speaker, we employ the iKinGazeCtrl module – a controller designed for iCub’s gaze, capable of independently steering the neck and eyes (Roncone et al., 2016) toward a point in the cartesian space. Additionally, our action module provides functionalities for controlling facial expressions (by activating LEDs) and synthesizing speech (by using Acapela Text-To-Speech⁶ with the child-like English voice “Josh”).

Self-Monitoring/State Controller This module acts both as Self-Monitoring and as State Controller. As a state machine, it is responsible for handling information coming in inputs and controlling the activation of other modules subsequently. For instance, it takes in input information coming from the *Sound Detection* module to manage the activation of the *Addressee Estimation* based on the start and end of the speaker’s utterance.

In parallel, it also monitors all the active modules of the architecture, providing such information to the *Visualization System* to be displayed on the tv-screen.

Visualization System An additional module of the architecture is the real-time visualization of the main processes involved in the proposed framework. This includes details about the robot’s current state, such as the activation of the

⁶<https://www.acapela-group.com/>

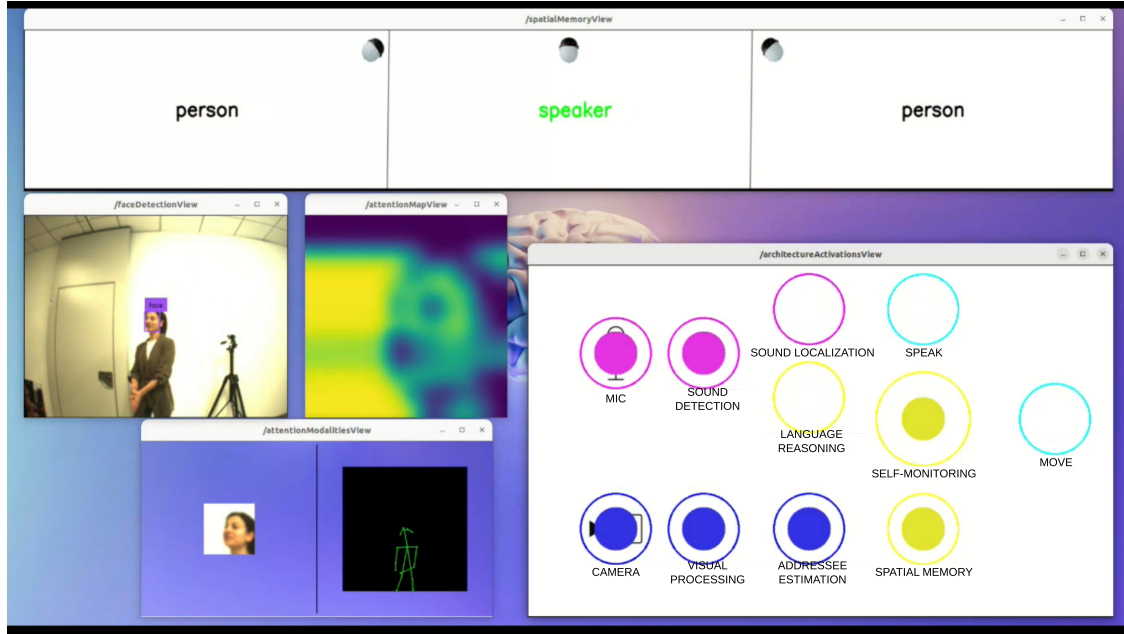


Figure 6: Screenshot of the visual explainability and transparency techniques that were shown on the screen behind the robot during the multi-party conversations. From top to bottom and from left to right: 1. visualization of Spatial Memory module; 2. camera stream with Face Detection information; 3. Attention Map showing the saliency of the input image of the XAE model; 4. the modular architecture with current activations displayed; 5. the relative contribution of the two inputs of the XAE model.

modular architecture, which illustrates the ongoing processes supporting the robot’s cognitive abilities. Additionally, it showcases the explainable and transparent solutions integrated into the XAE model. A 50-inch TV screen positioned behind the robot serves as a presentation board for various visualization windows (Figure 6).

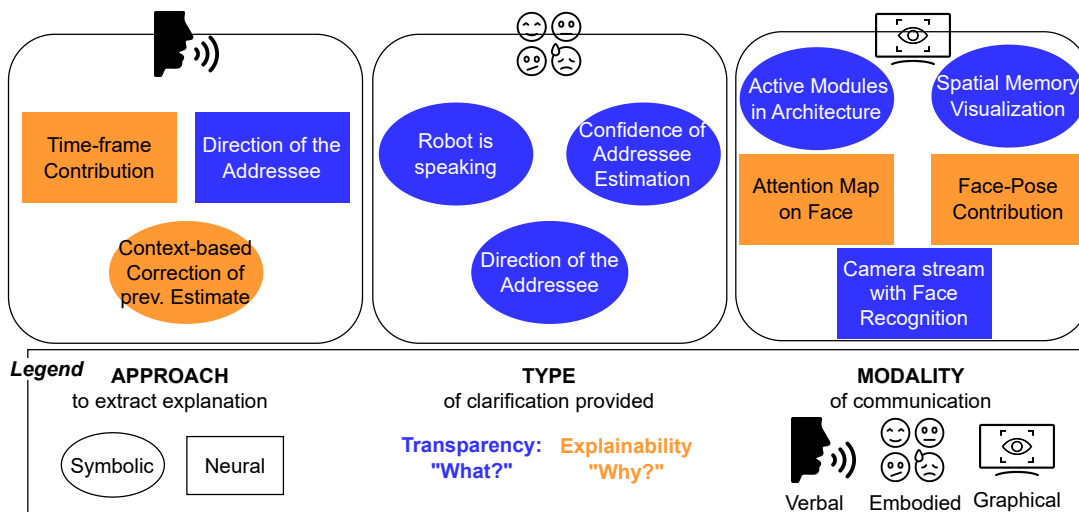


Figure 7: Illustration of our XAI framework. The explainability and transparency techniques we used in our system are ordered by approach (Symbolic or Neural), type of clarification (Transparency or Explainability), and modality of communication (Verbal, Embodied, Graphical).

Icons' attribution goes to Flaticon.com. Specifically, Verbal: Freepik; Emoticons: Khoirul Huda; Screen: Dmytro Vyshnevskyi; Eye inside the screen: Freepik

3.2.2 Evaluation of XAE model performance in real-time multi-party HRI.

In order to check the performance of the XAE deployed in real-time and, therefore, the actual AE capabilities of the above-mentioned architecture during multi-party HRI, we conducted an HRI evaluation study consisting of multiple sessions of interactions between three agents: the iCub robot and two humans. In each session, two researchers impersonated the characters of a fictional scenario in which a service robot (the iCub) was present (home, shopping mall, restaurant). 8 researchers (50% females) took part in the study, some of them acting in more than one session. We recorded a total of 122 utterances.

The robot’s behavior was managed by the architecture described in Section 3.2.1. The ground truth of the addressee was logged during the experiment by an operator who observed the interaction. For each utterance, the operator logged the addressee (robot or right or left) using the buttons of a GUI designed for this scope.

To evaluate the AE performance of the architecture, for each utterance we collected data coming from different modules: *Sound Detection*, *Sound Localization*, *Addressee Estimation Speech-To-Text*, and *Speech Generation*. After the experiments, data were automatically assembled together with the ground truth by using information from the system timestamps.

To overcome unbalance in class representation (the class “robot” was represented 64.75% of the utterances, whereas “right” and “left” 18.86% and 16.39% respectively), we used a weighted F1 score as a performance indicator. We evaluated the recorded experimental data about the addressee estimation at the different stages of the architecture. Firstly, we evaluated every output of the XAE model considering all its predictions separately (the XAE is programmed to provide an output every 0.8 seconds. Secondly, we evaluated only the final prediction of each utterance, as this is the prediction the robot uses to determine its behavior. Lastly, we recalculated the AE performance, taking into account corrections made by the Spatial Memory (e.g., if the prediction was ‘left’ but no one was found on the left, the robot considered itself the addressee).

We approached AE primarily as a Computer Vision problem, although, as humans, we also rely on syntactic and contextual clues within the message to infer the recipient. While we intend to explore the integration of both visual and semantic information to enhance the robustness of the AE model in future work, we analyzed whether, and with what performance, AE could be solved solely as a linguistic problem. We adopted a binary approach to determine whether the addressee of each sentence was either ROBOT or NOT-ROBOT. We evaluated three different models: Llama3 by Meta, GPT-3.5-Turbo by OpenAI, and Mistral7b by Mistral AI. Each model was tested with sentences from the conversation of the evaluation study, using both the context prompt employed in the actual interactions and an analysis prompt (refer to “LLM-based AE Predictions Context” in the Appendix C). To ensure a fair comparison with the vision-based system, we did not provide the LLM with the chat history, ensuring that the final decision was based solely on the current sentence and the context prompt. Given the inherent randomness in language models’ responses, we considered the average response over 10 iterations for each sentence. Additionally, we repeated the same analysis excluding sentences with explicit references to the addressee’s name (e.g., “Hello Mike, how are you?” or “Hi, iCub, can you help me with this?”). As a baseline for the Vision approach, we aggregated the left and right classes as NOT-ROBOT and we computed a weighted F1-score on the same binary classification as the LLMs’ task.

3.2.3 Development of a multi-modal Explainability and Transparency System

To implement a transparent and explainable modular architecture, we developed a framework providing several real-time clarifications about the processes and functionalities of the robot. To this aim, we use diverse techniques (see Figure 7).

Specifically, our solutions are the result of two possible *approaches to extract explanations* (Kerzel et al., 2022): neural or symbolic. The former approach leverages neural network outputs to extract information, whereas the latter represents the information about the system’s behavior with a symbolic code specified by the developer.

Another important difference is related to the *type of clarification provided*, which is rooted in how some literature differentiates between the concepts of explainability and transparency (Ciatto et al., 2020; Miller, 2019). Several accounts we implemented provide the reason behind the decision of the robot (explainability), whereas others describe the current functioning of the robot (transparency). The former answer the question “why is it happening?”, the latter reply to the question “what is happening?”. Following this classification, we implemented four explainability and seven transparency solutions for the human-robot interaction phase.

Eventually, several *modalities of communication* are exploited: verbal, embodied, and graphical.

Figure 6 shows a screenshot of the five techniques implemented via the graphical modality and displayed in real-time on the screen behind the robot. Two out of these five represent functional aspects of the architecture, i.e., how the architecture is working in terms of current activations and current information in memory. The Spatial Memory provides a 3-bin scheme with instances of people perceived and remembered by the robot, their (robot-centric) position, and

conversational role. An additional solution shows the scheme of the robot’s modular architecture onscreen, with real-time information about the current activations for each robot’s ability.

The other three graphical representations are implemented as streams of features the robot is paying attention to. The visual streams show, therefore:

- the processed output of the iCub’s right camera with bounding box information of detected faces;
- the attention map of the speaker’s face providing information about the salient part of the input image processed by the XAE model;
- the two inputs of the XAE model (the speaker’s body pose and face image) displayed with size changing in real-time proportionally to the relative importance of their contribution to the final output.

Other explainability and transparency techniques designed to clarify the addressee estimation process were implemented via the verbal modality. For instance, at the end of other speakers’ utterances, the robot provides an explanation for its final estimate of the addressee, saying that its decision relied on the speaker’s non-verbal behavior and, more specifically, which part of the speaker’s utterance (beginning, end, or the middle) impacted most on the final estimate. This enhances the transparency of its subsequent action (turning toward the addressee vs replying to the speaker). Moreover, the robot can correct any evaluation errors made by the XAE model after exploring the environment (e.g., if there is nobody in the estimated direction), and verbally clarify the correction.

Finally, we designed specific actions for the iCub’s facial expression to increase the understandability of the robot’s behavior via an embodied modality. iCub is endowed with face LEDs (eyebrows and mouth) that can change color and position and are synchronized with the speech synthesizer. We specified the iCub mouth (happy or neutral) to be coherent with the confidence of the estimate (happy for confidence over 80%, neutral otherwise). The color of the LEDs indicates the conversational role of the robot, consistent with the colors displayed in the spatial memory (green for “speaker”, red for “addressee”, and white otherwise). The movement of the eyebrows is meant to suggest the direction “left” or “right” of the estimated addressee (see video for clarification).

3.3 User Evaluation of the Explainability and Transparency System: Online User Study.

After developing the XAE model and integrating it into the robotic architecture, we ran a user study to assess external users’ perception of the Explainability and Transparency System described in the last Section.

Video Recordings We recorded a video of multi-party conversations with the robot⁷ and uploaded it on the soSci Survey⁸ platform for questionnaires delivering. In the video, the experimenters stage 3 different conversational scenarios, namely interacting with a social robot assistant in a shopping mall, a restaurant, and a domestic setting. Upon receiving the speaker’s position and gazing toward them, the robot utilizes the XAE model to estimate the intended addressee. In the case the estimated addressee is the robot, it replies to the speaker using the Speech Generation module. To ensure meaningful dialogues, we provided the LLM with context prompts tailored to each scene.

Participants were also given an extra introductory video clip to familiarize them with the visual solutions of the Explainability and Transparency System. The video shows the conversational interactions from an external perspective, with the robot in the middle (Figure 8). To increase the visibility of important features, we incorporated a zoomed-in view of the robot’s face in the bottom left corner, along with the robot’s visual explanation system in the bottom right corner of the screen (Figure 6). Participants were instructed to focus on both the overall scene and the robot’s explanations.

Demographics We performed an online user study with 60 participants (76% female) with naive users. We designed the survey on soSci⁹ and administered it through Prolific. Participants received a compensation of £9.00 per hour. All participants gave informed consent about collecting and analyzing data anonymously. The study was approved by Comitato Etico Regione Liguria.

Questionnaires After viewing the videos, participants were given 7-point Likert scale questionnaires about their perceptions of the robot, and their impressions about the clarifications provided by the implemented Explainability and Transparency System. For the robot’s perception, we used items regarding its Warmth and Competence (Fiske et al., 2007), Likeability (adapted from Spaccatini et al. (2019)), Experience and Agency (Gray et al., 2007), and Cognitive and Affective Trust (Bernotat et al., 2021). Moreover, we asked them to rate their Satisfaction with the Explanations

⁷The entire video can be found at the following link <https://www.youtube.com/watch?v=zZF-L0gtRu4>

⁸<https://www.soscisurvey.de/>

⁹www.soscisurvey.de



Figure 8: A frame of the multi-party conversation between the robot and the three actors. iCub is expressing a doubting face because it is estimating the addressee of the speaker in front of it; its LEDs are white because it has no role in the current dialogue. Behind the robot, we can see the screen displaying the graphical explainability and transparency techniques (Figure 6).

(Hoffman et al., 2018), and their perceived Usefulness and Intrusiveness (Conati et al., 2021). We asked the participants to individually evaluate the various explanation modalities (verbal, embodied, and graphical), also with open-ended questions, to gain a complete understanding of their perception of each.

Statistical Analysis Data obtained from questionnaires have been analyzed in Jamovi Software v. 2.4.11 (The jamovi project, 2023) using Mixed Models (Gallucci, 2019), Spearman Rank Correlation, and Conditional Mediation analysis (Gallucci, 2020).

Each of the three XAI parameters (Satisfaction, Usefulness, and Intrusiveness) were employed as the dependent variable in a Mixed Model that computed statistical differences between the three explanation modalities (factor). Participants' ID was applied as a random effect to adjust for each participant's baseline and model the intra-subject correlation of repeated measurements. Bonferroni correction has been applied to assess post-hoc pairwise comparisons between the explanation modalities.

Moreover, we conducted Spearman rank correlation tests to investigate the relationship between the three parameters used to assess participants' evaluation of explanation modalities from the user perspective. For this test, we analyzed the three explanation modalities independently.

To assess the extent to which the robot's explanations of its behavior contributed to building participants' trust, we examined the relationship between the usefulness of these explanations and the two components of trust: affective and cognitive. To this aim, we performed two tests using Conditional Mediation analysis, one for each component of trust. Affective Trust and Cognitive Trust were used as the dependent variable of the analysis, while Usefulness acted as the covariate. We tested such relationships using the robot's qualities evaluated by participants in the survey as Mediators (Perceived Warmth, Experience, Agency, Likeability, and Competence). In addition, we employed the explanation modality as a Moderation Factor to assess the extent to which each of them contributed to the building of trust.

		predicted class					predicted class		
		robot	left	right			robot	left	right
real class	robot	75.54%	13.91%	10.55%	real class	robot	74.74%	11.34%	13.91%
	left	14.48%	81.30%	4.22%		left	12.71%	81.05%	6.23%
	right	14.54%	6.08%	79.38%		right	12.71%	6.08%	81.21%

Figure 9: Confusion matrices for the IAE (left) and the XAE (right) model.

4 Results

4.1 Evaluation of the AE models.

4.1.1 Performances of the improved AE and XAE models and comparison with SOTA baseline

To provide a statistically robust evaluation of our proposed models (IAE model as well as the XAE model), the training is repeated five times in total for each test set, using different random seeds. The two models achieve comparable accuracy. The IAE model reaches 79.51% average F1 score with a standard deviation of 0.56%, whereas the F1 score for the XAE model is 79.40% with a standard deviation of 1.06%. Thus, both models surpass the previous SOTA F1 score of 75.01%, described in Mazzola et al. (2023), by $\approx 4.45\%$. When looking at their confusion matrices (Figure 9), we see that the models have roughly equal distribution of each type of misclassification. We also see that the models are slightly weaker on recognizing the cases when the addressee is the robot.

To test our XAE model’s capabilities on recordings captured using the iCub, we first analyze its accuracy on the data provided in Saade (2023) (further referred to as the iCub data). We trained the XAE model on the Vernissage corpus and tested it on the iCub data, with resulting testing accuracy of 66.31%. This informs us that even though the data distribution is quite different from the Vernissage dataset, the model can successfully estimate the correct addressee most of the time. However, the performance is still notably worse than on the Vernissage data. Thus, to ensure the best possible accuracy of the model when deployed in the iCub, the final model used in the user study was trained on both of the datasets.

4.1.2 Ablation studies

As there can be three different attention modules in our network, XAE and IAE can be seen as two possible extremes – all attention modules on, or all off. However, we can treat them independently, getting six new combinations, and, therefore, six more networks to analyze. By doing this, we get more insight into the contributions of individual attention modules.

For each of the additional networks, we performed a hyper-parameter search similar to the one done with XAE. All the searched parameters and the optimal values are displayed in Table 5, along with F1 scores and standard deviations, computed across 5 different random initializations.

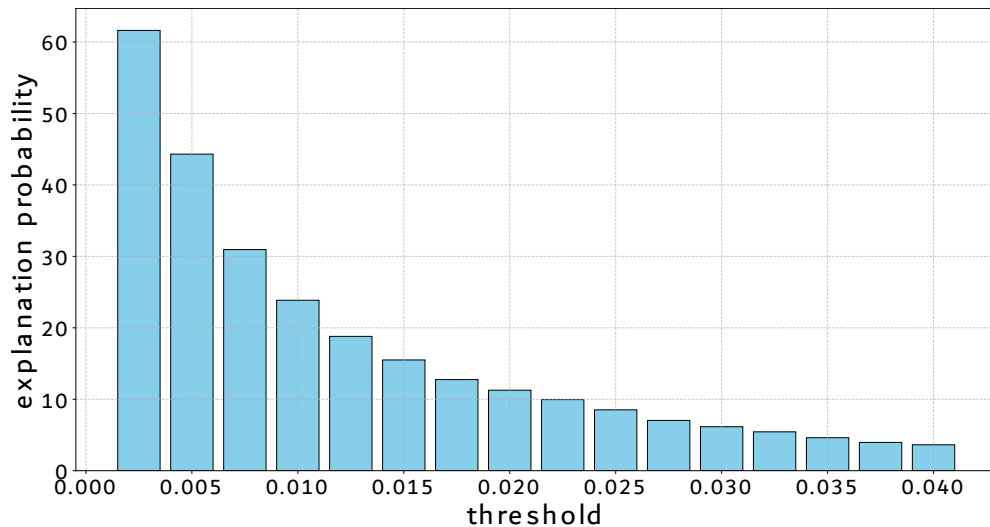
As we can see, all the analyzed networks achieved very similar F1 scores, comparable with the performance of IAE and XAE models. However, the hyper-parameter values differ greatly, meaning that each of the networks can perform well, if a proper hyper-parameter search is conducted. Otherwise, the performance may suffer.

4.2 Quantitative assessment of Explainability in XAE model

When analyzing the distribution of the face vs. pose attention weights, we found that the face and pose information is almost always equally important, i.e., the average score is 0.5. Our resulting XAE model achieves an average score of 0.5 and deviation of 0.04. On the other hand, we notice a negative correlation of -0.87 ($p = 0.001$) between the dimensionality we use for the face and pose embeddings and the logarithm of the importance deviations. The higher the dimensionality, the lower the deviation of attention scores (the lower the distinction rate between the two modalities). Thus, during the optimization process, it is not enough to optimize the model only for the performance, but also for the expressiveness of the explanations, like the deviation of importance scores in this case.

Table 5: Optimal hyper-parameter values and resulting performance of networks analyzed during the ablation studies. First three columns describe the networks.

Attention modules			Hyper-parameters										F1	std
M1	M2	M3	act3	act4	e-dim	out1	out2	out3	opt3	dim_qk	dim_in	dim_v		
off	off	on	-	Tanh	-	37	23	20	-	-	-	53	79.8	0.787
off	on	off	ReLU	-	-	158	out1	58	Adam	83	116	-	80.0	0.643
off	on	on	Tanh	Tanh	-	152	out1	53	SGD	90	129	63	81.5	0.428
on	off	off	-	-	30	75	19	59	-	-	-	-	80.5	0.609
on	off	on	-	Tanh	180	16	14	22	-	-	-	102	78.4	1.414
on	on	off	ReLU	-	66	13	out1	40	SGD	167	24	-	79.1	0.765

Figure 10: The influence of threshold value (x -axis) on the probability (y -axis) of a verbal explanation being triggered at the end of a sequence.

Our experiments also showed that in some cases of networks with lower dimensionalities of the face and pose embeddings, the explanation capability seemed to increase, and the pose information was slightly prevalent.

To further explore the properties of our XAE model in greater detail, we analyze time frame scores with 10-frame-long sequences of the Vernissage dataset. A way to look at the activations is to compute their distribution. When considering only the stack of values independently, they precisely follow a Gaussian distribution with a mean of 0.1 and standard deviation 0.0055. Our explanation of the low deviation is that since there are only 10 frames in each sequence, they do not capture a long period of time; thus, their embeddings are usually quite similar. We also observe that the weights change more in the case of frames with greater variability.

Next, we analyzed the threshold value for triggering an explanation at the end of a sequence. The threshold clearly influences the rate at which the verbal cue is generated. In Figure 10 we can see the probabilities of triggering a verbal response for differing threshold values. We empirically verified that threshold values higher than 0.02 yield verbal cues aligning with human expectations. In contrast, by using lower values, the noise patterns sometimes overrule the useful information, yielding responses that are difficult to verify.

4.2.1 Comparison of ViT attention maps with Grad-CAM

Even though using our XAE model we can extract the inherent attention maps of the vision transformer to produce explanations, there are means to generate similar saliency maps for other model families, such as CNNs, present in the baseline model. One such method is the Gradient-weighted Class Activation Mapping (Grad-CAM) proposed by (Selvaraju et al., 2017), which computes the weighted activations, usually of the last convolutional layer, upsampled to the input space.

In Figure 11, we see four examples of the importance of face in the baseline model and the explainable model. In general, the saliency maps of the XAE model are visually more appealing than those produced using Grad-CAM (in the IAE model), yet it is important to consider all factors influencing the quality of the maps. Each method has its own set

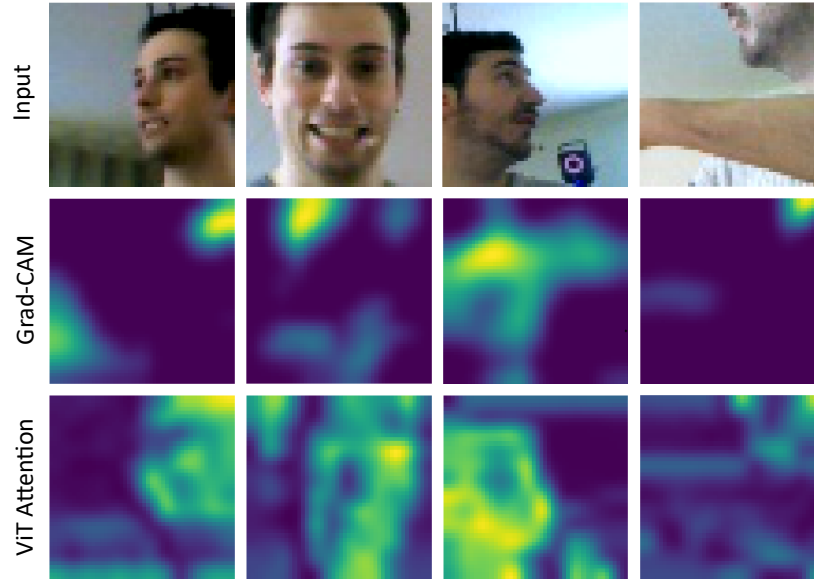


Figure 11: Comparison of saliency maps in IAE and XAE model. In the former, we employ Grad-CAM to approximate the importance of image regions, whereas in the latter, the important image parts are taken from the attention mechanism present in the ViT.

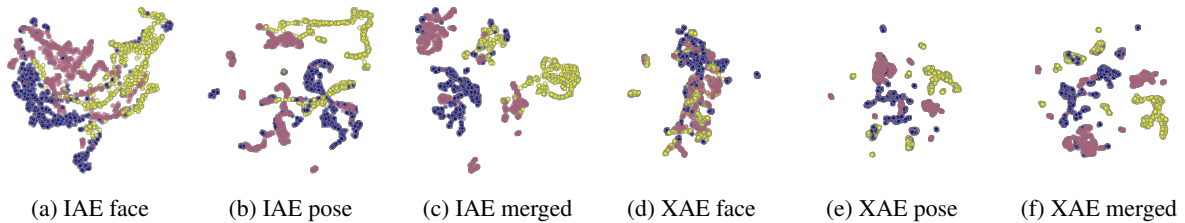


Figure 12: 2-dimensional UMAP embeddings of face, pose, and their merged latent representations formed on the baseline model (top) vs. the explainable model (bottom). The individual colors demonstrate the labels of the individual inputs (blue=left, purple=right, yellow=robot).

of hyperparameters, and lacking a fool-proof numerical evaluation of the explanation quality, it can be difficult to pick the best ones.

4.2.2 Face vs. pose expressiveness in IAE and XAE models

To further compare the properties of the XAE model with the IAE model, we analyzed the high-dimensional embeddings of face, pose, and their combination (in the case of IAE, their concatenation), using Uniform Manifold Approximation and Projection (UMAP) (McInnes et al., 2018).

Our goal is to consistently compare the representations of data embeddings while keeping in mind that high-dimensional spaces often obstruct fair comparisons. Therefore, using UMAP, we transform the inner activations of the input into two-dimensional space. We first empirically set the main UMAP parameters (minimal distance in the output space as 0.7, and the number of neighbors which contribute to the final approximation as 20) to produce embeddings that are neither too stretched nor completely mixed. Then, for a given test set, we collect all face, pose and their respective merged embeddings, and project them to 2D space separately. The resulting 2D projections are shown in Figure 12, where we project the embeddings in the IAE and XAE models. There we see that the face embedding is not very clumped to each other in general, which means that the data is more variable. To numerically assess the data structure after the UMAP projections, we compute the ratio of inter-class to intra-class distances. In figure 13, we plot this ratio for the IAE and the XAE model, for three randomly picked test-sets. We see that the XAE model has a higher ratio in the case of the face embeddings. This can be understood as face embeddings being quite complex when processed by the XAE model.

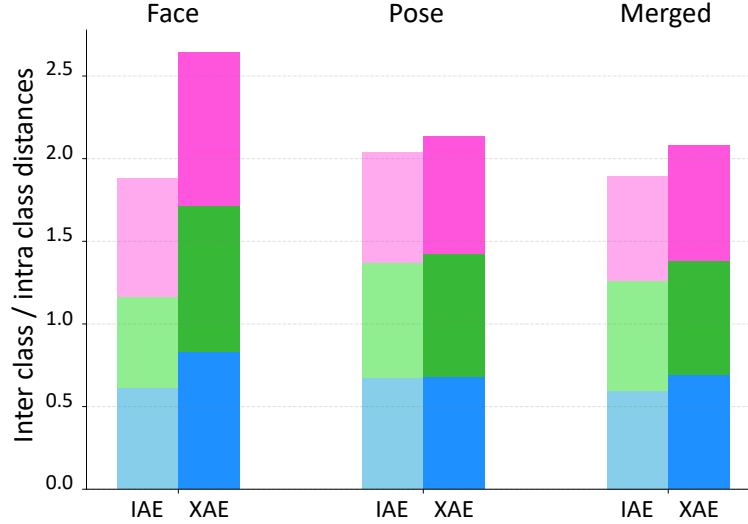


Figure 13: Development of ratio of inter-class to intra-class distances of face, pose, and their merged embeddings in IAE and XAE networks. Individual colors represent three (out of ten) randomly picked test sets used for the measurements.

4.3 Evaluation of the modular architecture in real-time HRI.

To measure the performance of our architecture in AE, we analyzed the results of the HRI evaluation study as reported in Section 3.2.2.

Considering all the predictions across all utterances for all experimental trials, the XAE model achieved a weighted F1-score of 85.56%. Figure 14.A shows the confusion matrix, which reports the performance (recall) for each class. The figure shows an overall good accuracy with left and right classes performing better than the robot one (76.42% for the robot class, 97.56% for the left class, and 94.44% for the right class). This demonstrates the validity and robustness of our approach also in real-time interaction scenarios.

A. Performance on all Predictions			B. Performance on Utterances (no spatial memory info)			C. Performance on Utterances (with spatial memory info)								
		predicted class					predicted class					predicted class		
		robot	left	right			robot	left	right			robot	left	right
real class	robot	76.42%	7.32%	16.26%	real class	robot	70.89%	5.06%	24.05%	real class	robot	79.75%	3.80%	16.46%
	left	0.00%	97.56%	2.44%		left	0.00%	95.24%	4.76%		left	0.00%	95.24%	4.76%
	right	0.00%	5.56%	94.44%		right	0.00%	4.76%	95.24%		right	0.00%	4.35%	95.65%

Figure 14: Confusion matrices representing the performances (recall) of the architecture with the deployed XAE model in the multi-party HRI evaluation study. Figure A represents the performance computed on all predictions of the XAE model (each utterance can lead to one or more predictions). Figure B represents the performance considering only the final estimate of XAE for each utterance. Figure C represents the performance on each utterance considering the correction made by the spatial memory module.

However, the robot's behavior is ruled only by the final estimate of each utterance, so that the robot answers to the utterance in case of "robot" prediction" or turns left or right otherwise, in search of the predicted addressee. For this reason, it was essential to measure the performance of the XAE model only considering the final estimate. Figure 14.B shows the confusion matrix for the selected instance of the AE. The weighted F1-score computed on all utterances is 80.64%. In this case, the accuracy of the robot class went slightly lower to 70.89%, whereas the "left" and "right" classes maintained a similar score.

This estimate does not consider the spatial memory module, which is updated based on the people detected and remembered in the environment. Therefore, the very final AE from the architecture is the one with the applied corrections after considering the context from the spatial memory. Figure 14.C shows the accuracy of this final estimate.

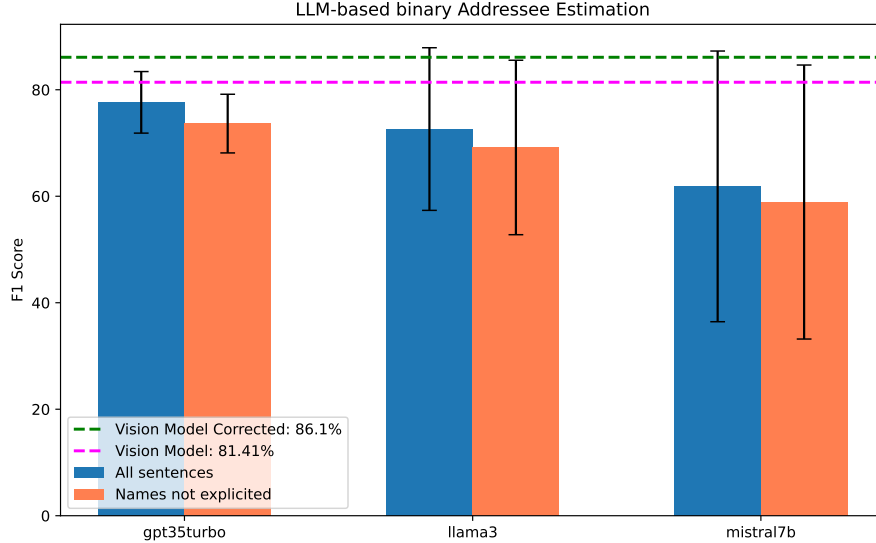


Figure 15: Average weighted F1 scores for addressee prediction using three different LLMs, based on conversations from the HRI evaluation study. For comparison, the corresponding metrics for the vision-based model are also reported, both with and without spatial memory correction.

In the figure, an improvement in the estimation of the robot class is noticeable (79.75%), which demonstrates a crucial role of the modular architecture in solving the AE task.

To assess whether the CV approach could be replaced by a linguistic approach with LLMs, we evaluated the performance of different families of LLMs in a binary task for predicting the correct addressee (ROBOT vs NOT-ROBOT) for conversations in the HRI evaluation study. We found that, on average, none of the three tested LLM outperformed the vision system (see Figure 15). In the same task, our XAE model achieved a weighted F1-score of 81.42% on utterances, which increased up to 86.09% with the correction of the spatial memory. On the other hand, the best LLM we tested is GPT-3.5-Turbo with an average F1-score of $77.6 \pm 5.8\%$, followed by llama3 ($72.6 \pm 15.5\%$) and Mistral7b ($61.8 \pm 25.4\%$). Furthermore, when considering only sentences with no explicit reference to the addressee’s identity, the LLMs performance drops further (F1-score of $73.6 \pm 5.5\%$ for GPT-3.5-Turbo, $69.2 \pm 16.4\%$ for Llama3 and $58.9 \pm 25.7\%$ for Mistral7b).

4.4 User Evaluation of the Explainable and Transparent System

Table 6: Statistics referring to participants’ evaluation of the robot’s Explainability and Transparency System for different modalities of communication (verbal, embodied, graphical).

Method	Satisfaction		Usefulness		Intrusiveness	
	Mean	SD	Mean	SD	Mean	SD
verbal	5.26	0.89	5.04	1.22	2.80	1.66
embodied	4.30	1.37	4.38	1.66	2.63	1.61
graphical	5.03	1.42	4.74	1.74	3.28	1.91

Table 6 reports the means and standard deviations of three questionnaire scales (Satisfaction, Usefulness, and Intrusiveness) grouped by the three explanation modalities (verbal, embodied, and graphical). The Mixed Models analysis (see 3.3 for test description) revealed a significant Fixed effect of the modality on Satisfaction ($F(2,118)=20.6$, $p < 0.001$), Usefulness ($F(2,118)=9.24$, $p < 0.001$) and Intrusiveness ($F(2,118)=4.62$, $p=0.012$). After post-hoc pairwise comparisons with Bonferroni correction, participants were found more satisfied with Verbal ($M=5.26$) and Graphical modalities than with the Embodied one ($M=5.03$) (Verb-Emb: $B=0.968$, $t(118)=6.16$, $p < .001$; Graph-Emb: $B=0.729$, $t(118)=4.64$, $p < 0.001$), as shown in Figure 16. Concerning Usefulness, participants found more useful the Verbal (5.04) than the Embodied modality (4.38) (Verb-Emb: $B=0.661$, $t(118)=4.30$, $p < .001$) and more Intrusive the Graphical than the Embodied modality (Graph-Emb: $B=0.650$, $t(118)=2.94$, $p=.012$). The other comparisons were not found to be significant in a post-hoc test.

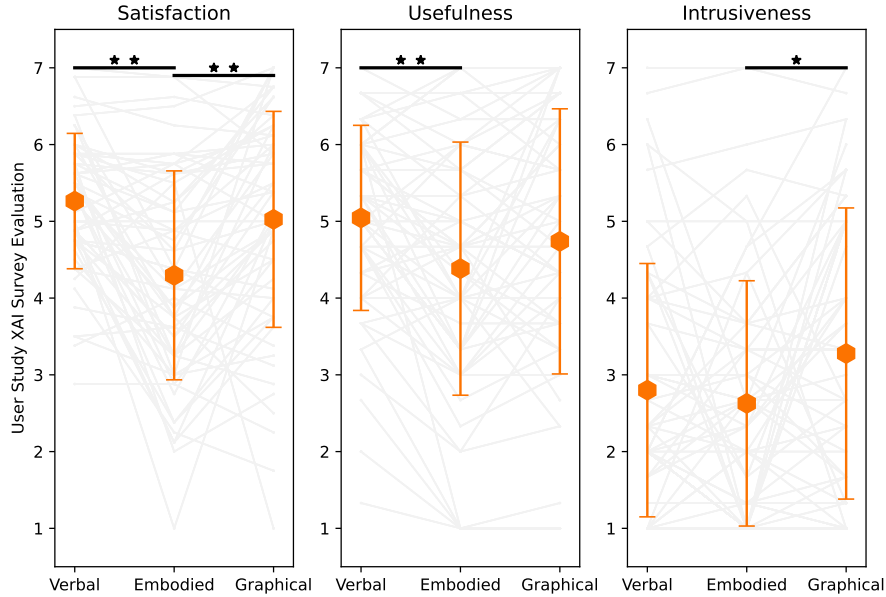


Figure 16: Plot of the Mixed Model on explanations’ Satisfaction, Usefulness, and Intrusiveness. The orange hexagons represent the means of all modalities. Error bars are computed with SDs. Grey lines connect repeated measures for each participant, which in the Mixed Model are considered as a random effect. * refers to $p < 0.05$ and ** to $p < 0.001$.

In the Appendix D, Tables D.1, D.2, D.3 present all the results from Spearman Rank Correlations tests computed on the three parameters (Satisfaction, Usefulness and Intrusiveness). It is interesting to notice that for all modalities we found a strong positive correlation between Usefulness and Satisfaction. Moreover, a negative correlation was also found for all modalities between Satisfaction and Intrusiveness.

To further analyze participants’ feedback provided in the online survey, we conducted a Conditional Mediation analysis, quantifying the extent to which the robot’s qualities evaluated by participants (Competence, Likeability, Agency, Experience and Warmth) mediated the relationship between the perceived Usefulness of explanations and the trust toward the robot, and whether the explanation modalities (verbal, embodied, graphical) moderated such relationships. The path diagram in Figure 17 displays the relationships and types of effects between the variables as assessed in the Conditional Mediation test. Overall (i.e., when averaging the effects associated with each explanation modality), we found a total effect (i.e., the combination of the direct and indirect effects) of Usefulness on both components of trust (on Affective Trust: $B = .42$, $SE = .05$, $p < .001$, 95% CI = [.33, .51]; on Cognitive Trust: $B = .31$, $SE = .04$, $p < .001$, 95% CI = [.24, .38]). In regard to the relationship of Usefulness toward Affective Trust, we found a statistically significant effect both directly ($B = .10$, $SE = .05$, $p = .03$, 95% CI = [.01, .19]) and indirectly. In this case, the test revealed a mediation of the robot’s Agency ($B = .07$, $SE = .03$, $p = .02$, 95% CI = [.01, .12]), Competence ($B = .15$, $SE = .04$, $p < .001$, 95% CI = [.07, .24]) and Warmth ($B = .09$, $SE = .04$, $p = .02$, 95% CI = [.01, .16]). With respect to the relationship of Usefulness toward Cognitive Trust, the analysis revealed a direct effect ($B = .20$, $SE = .04$, $p < .001$, 95% CI = [.11, .28]) combined with an indirect effect mediated by the robot’s Warmth ($B = .10$, $SE = .04$, $p = .008$, 95% CI = [.03, .17]). Moreover, as mentioned above, we also investigated the Conditional Mediation effect associated with each explanation modality, which we included in the Appendix D (Tables D.6 and D.7).

5 Discussion

This study is guided by the effort to put into action transparency and explainability techniques in a social robot with multi-party conversation abilities. To this aim, we designed and applied XAI solutions to a real-time human activity recognition model for the estimation of the addressee and implemented it in a modular robotic architecture for multi-party conversation together with other transparency solutions to show the underlying processing of the robot’s behavior.

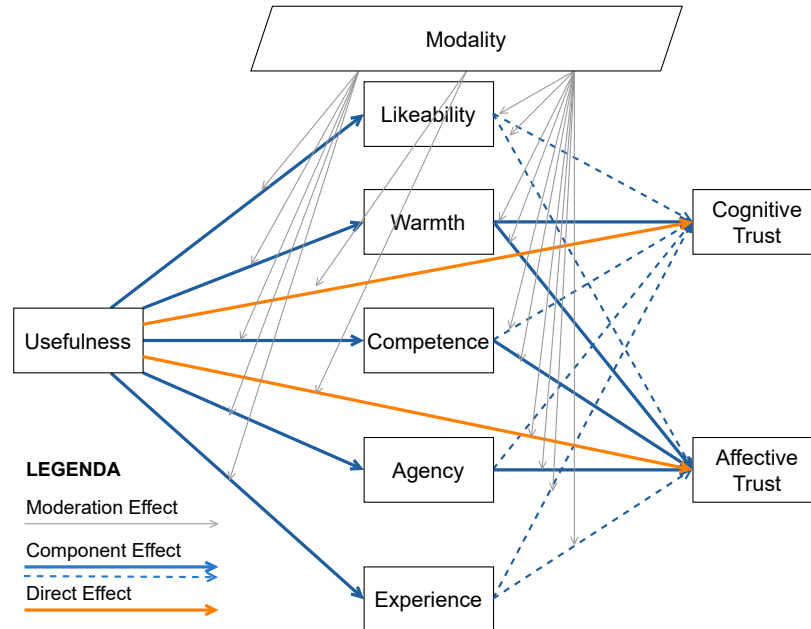


Figure 17: Path diagram of the Conditional Mediation analysis. The independent variable (or predictor) is the perceived Usefulness of explanations while the dependent variables are Affective Trust and Cognitive Trust. This relationship is mediated by participants’ evaluation about several robots’ qualities (Likeability, Warmth, Competence, Agency, Experience) and moderated by the three explanation Modalities (verbal, embodied, graphical). The solid orange and blue arrows represent, respectively, the significant direct and indirect (in the case of both components) effects of Usefulness on Trust.

5.1 The explainability of our models

Our ablation studies showed, that it is possible to train an addressee estimation network with a reasonable performance, regardless of which parts (M1, M2, M3) of the network are taken from the XAE architecture (explainable), and which from the IAE architecture (not explainable). Therefore, the choice of M1, M2, M3 can be used to regulate the explainability of the network. Thanks to the fact, that all tested networks achieved comparable performance scores, the choice of architecture depends only on the desired level of explainability. However, as explainable options are computationally more complex, it should be advised to use the simpler, not explainable version, in case the explanations are not needed at all.

When analyzing the heatmaps produced using Grad-CAM and those extracted from the XAE model, we saw that the XAE model usually produces clearer saliency maps that more correspond to the face location. Our hypothesis as to why the inherent explanations are better is due to the complex model architecture. Grad-CAM requires full gradient information computation for a correct estimate of the saliency map, but the gradients of a recurrent network can be relatively imprecise. Another benefit of computing the explanations on the XAE model is the computational efficiency. In addition to the inference, we only need a fraction of computational time since we only extract the already calculated attention scores. On the other hand, the Grad-CAM can be more tricky and it requires the gradients to be computed w.r.t. the last convolutional layer.

During our analysis of the hidden representations of face, pose, and merged information using the UMAP projection method, we found some differences between the XAE and IAE models. For example, the explainable model tends to create more separate point clusters (mainly of pose and merged embeddings), whereas the face embeddings are more entangled, and individual class instances are close to each other. Besides visual assessment of the produced projections, we also employed the computation of inter-class vs intra-class distances, that confirmed the observed variability of class separability, especially in the face representations.

Perhaps one of the greatest challenges is quantifiable explanation evaluation. To properly assess the level and usefulness of individual explainability methods, three main evaluation directions are often pursued: application-grounded, human-grounded, and functionally-grounded (Gilpin et al., 2018). The first two involve human participants who provide

meaningful feedback (i.e. in various user studies), which is later analyzed. However, the functionally-grounded evaluations are inherently difficult to achieve. There, the goal is to formulate a formal definition of explainability and a rigorous mathematical measure that produces quantitative outputs. For this reason, we have mostly focused on evaluating the quality of explanations by user studies.

5.2 The real-time implementation in the architecture for multi-party conversation

Built with a modular approach, our architecture was designed as the mean to connect our XAE model with the other modules necessary for the task of multi-party conversation: from Sound Detection to Spatial Memory and Speech Generation. At this stage, our architecture only missed a sound localization module, which the experimenter handled with the Wizard-of-Oz technique. Beyond that, the interaction flow was smooth and autonomous, as presented in the video.

Results from the HRI evaluation study highlighted a successful deployment of the XAE module in real-time interactions. The model was demonstrated to be robust, maintaining consistent performances with respect to the previous testing phase (see Section 4.1). In line with that, the model achieved better results for the left and right classes, confirming higher sensitivity in detecting poses and faces directed toward these two directions, whereas the accuracy dropped in the case of the speaker addressing the robot. This is particularly evident when computing the F1-score on the XAE final estimates, provided at the end of speakers' utterances. Nevertheless, that is also the case in which the deployment of the XAE module in the modular architecture demonstrates to be fruitful. Thanks to the constantly updated spatial memory information, almost 30% (7 on 24) of the wrong XAE predictions have been corrected, significantly improving the accuracy for the robot class and leading to an overall weighted F1-score of 86%. More importantly, thanks to such corrections, the flow of interactions did not break, with the robot that was enabled to answer participants' questions when addressed.

We decided to solve the AE problem with a CV approach because, as evidenced in previous literature (Skantze, 2021), meaningful information about the direction of the addressee are hidden in the speakers' non-verbal behavior, specifically their gaze and body pose. To leverage such clues, we opted for processing both the image of the speakers' faces and the coordinates vectors of their body joints. A different approach could be used, though. Information to estimate the addressee identity, albeit not their relative position in the space, might be contained also in the semantics of the utterance. It was therefore important to check whether such information is sufficient at least for a binary estimate (robot vs. somebody else) and, in this case, if the visual processing is redundant for this scope. To address this question, our analysis with different LLMs demonstrates that a purely linguistic approach for addressee prediction performs worse compared to the vision-based approach. Furthermore, as expected, performance decreases even further in cases where the addressee's name is not explicitly mentioned, which is a common scenario in real-world applications. In other words, while semantic information serves as an important cue for addressing the problem of addressee estimation, it is often insufficient and not consistently reliable. A holistic approach that combines both types of observations and assigns greater weight to the one with higher confidence would be the optimal solution. To this end, we are actively developing a more advanced version of the proposed architecture that integrates behavioral and linguistic cues. This improvement is designed to provide greater robustness in handling complex and dynamic interaction scenarios, particularly those marked by high levels of uncertainty.

Another positive element about our approach is that, given the XAI techniques and system implemented in our architecture, the predictions of the robot are made less opaque, granting the user a greater awareness of the features and motivations underlying the robot's behavior in real-time. That would not be the case with LLMs providing explanations that, besides being post-hoc, could also be verbose and reflect problems that LLMs still face, such as hallucination (Tonmoy et al., 2024) and inaccuracy in reflecting the model's internal reasoning (Agarwal et al., 2024).

A modular design for the multi-party conversation architecture was preferred to an end-to-end approach for two reasons. First, multi-party conversation is a complex scenario involving various activities and multiple individuals interacting simultaneously. A modular approach offers greater controllability of the robot processes and behaviors in such unpredictable contexts. Second, real-time multi-modal processing allows to exploit the synergy of different modules, enabling them to self-supervise each other and correct any erroneous estimates.

As it is visible in the recorded multi-party interactions, the XAE model failed twice, but thanks to the modular approach, these errors could be amended, and the conversation resumed correctly. For instance, thanks to Speech Understanding and Generation modules, when iCub is told the utterance was addressed to someone else, it apologizes for interrupting.

The connection with spatial memory is another pivotal point. Thanks to this module, the final estimate of the addressee is significantly improved because it is not only based on multiple features coming from the robot's vision but also on continuously updated spatial-contextual information of the environment, following a more cognitively-inspired approach.

Contextual information about people in the environment was used in previous works, but it was given as input to the neural network before the addressee estimation, without any possibility of updating it after the inference. Hence, to our knowledge, our architecture is the first that can 1) make corrections on the addressee identification based on additional exploration and spatial memory information and 2) discover new people and update the spatial memory based on the addressee estimation. For instance, in the first case, if the addressee is estimated to be on the speaker's left, but the robot doesn't detect anyone in that direction, it infers that the utterance was directed towards itself. On the other hand, in the second case, if the addressee is estimated at the speaker's left and the robot does not remember anybody in that direction, it turns its gaze to check over there and may detect new people.

5.3 The users' evaluation

The implementation of the XAI model in the robot's architecture for multi-party conversation aimed to enhance the comprehensibility of the robot's underlying processes. The system's opacity can be an obstacle to the perceived reliability of the robot (or any other artificial system) both for the users and its developers. Moreover, this issue becomes even more problematic when it comes to multi-faceted modular architectures, where several processes concur in executing a complex behavior (Wortham et al., 2017). To reach an efficient and smooth interaction, developers and HRI designers need certainly to take care of the robot's performance, but also of their user-friendly intelligibility (Sciutti et al., 2018). It is to ensure this understandability, and hence reliability, that we designed our framework and system to provide real-time clarifications of the robot's behavior and the processes underlying its functioning.

The act of explaining is a social mechanism: someone (the explainer) explains to someone else (the explainee) (Hilton, 1990). Recently, also the XAI community recognized and exploited this social component of the explainability problem, highlighting the explainees' needs within the explanation exchanges (Miller, 2019). The active role of the explainee has also been stressed by Rohlfling et al. (2021) in their co-constructive approach.

In our online user study, we presented multi-modal explanations to naïve explainees to assess their evaluation of the different modalities of the Explainability and Transparency System during some multi-party conversation scenarios. In this way, we aimed to quantify the explainability and transparency techniques deployed in the XAE model and in the whole robotic architecture from a user perspective, together with the users' perception of several features of the robot's appearance and behavior.

We found all participants were more satisfied with the verbal and graphical explanations than with the embodied ones (i.e., the ones expressing the model's estimates and confidence via the robot's facial expressions). This result may be due to the embodied behavior design choices that some users could have found less intuitive and expressive than expected. Such a result is in line with the Usefulness metrics, where the verbal modality was found more useful than the embodied one. Interestingly, the graphical modality was found more Intrusive than the embodied one. The positive feature of non-verbal behavior is that it does not hinder the flow of interaction since it does not cause any interruption in verbal communication nor shift the users' focus of attention as the screen with graphical information may do. Nevertheless, this study shows that an accurate design of the robot's behavior is required because the implicit nature of non-verbal behavior may be an obstacle to the comprehension of the information conveyed.

On average, our Conditional Mediation analysis highlights the importance of the perceived usefulness of explanations to building trust towards robots, both in an affective and a cognitive sense. No relevant differences among explanation modalities were observed in the analysis of the Usefulness-Cognitive Trust relationship. Here, Usefulness maintains both a direct effect and an indirect effect mediated by Warmth, across all modalities. Conversely, in the analysis of the Usefulness-Affective Trust relationship, some differences became noticeable across modalities. This is especially evident for the verbal modality with respect to the others (embodied and graphical). With the verbal modality, the relation Usefulness-Affective Trust is not direct (it is so in the other modalities) but mediated (more strongly than the other modalities) by some robot's qualities: Agency, Competence, and Warmth. We can, therefore, hypothesize that while all modalities contributed to the building of trust, the contribution of the verbal explanations passed (more heavily) through the characterization of participants' perception of the robot.

Participants' satisfaction with the explanations and their perceived usefulness correlated for all the modalities meaning that participants' appreciation came in general from a utilitarian viewpoint: the more useful, the more satisfying. This result is coherent with the declared objective of the user study since participants had to exploit the robot's explanations to make sense of its behavior. All the modalities also showed a negative correlation between Satisfaction and Intrusiveness, showing that Intrusiveness should definitely be taken into account when designing an XAI system.

Regarding the qualitative feedback provided by participants at the end of the survey, it is noteworthy that they never mentioned the robot's attention map in their open-ended responses. This suggests a reluctance to use that explanation modality, possibly due to difficulties in interpreting it.

Overall, these results demonstrate that explainability represents a crucial capability for robots employed in social environments: not only their competence but also how and why they come to a decision matters. This is the reason why we do not need to arouse a blind trust towards robots but a justified one, based on the people’s knowledge about robots’ hidden processes, also exploiting the robots’ embodiment (Matarese et al., 2021). Diversifying the explanation modalities is one of the ways to follow when implementing XAI systems, as we showed in this study.

5.4 Limitations and Future Improvements

Implemented in the whole modular architecture, the explainable addressee estimation model we designed in this work offers verbal and non-verbal (embodied and graphical) explanations alongside the classification of the addressee. However, it is important to address its limitations. Given the surprisingly high sensitivity of the frequency and quality of the explanation on the hyper-parameters, a simple error optimization may not guarantee the model to produce meaningful explanations. Therefore, it would be useful to devise a training method that aligns with achieving good accuracy and generates reasonable and discriminative explanations.

In this work, we diverged from the majority of the previous approaches, which employed a simple binary classification, detecting only if the robot is addressed or not. The main reason was to provide the robot with extra information about the relative position of the addressee (in case it is not the robot), to enable smoother interactions. Although our 3-class classification approach is more fine-grained, in-depth comparisons of accuracy with previous methods are difficult to obtain. In theory, our approach could be replaced by performing multiple binary classifications for each output category and pooling the individual outputs to produce the final decision. However, due to the final pooling step, interpreting ensemble classifiers is much less straightforward. Therefore, we opted for a single multi-class classifier, which enabled us to explore multiple different explanation methods.

Although the XAE model has proven to be robust to a different setting, real-world deployment may require training with additional data because the model performance heavily relies on the quality and representativeness of the dataset, which may not always align with real-world scenarios. Thus, to improve its adaptability to new scenarios and robustness to different settings, an advisable solution would be implementing continual self-supervised learning to allow the robot to increment its knowledge while interacting with humans. Moreover, the current design of the modular architecture is not yet ready for exploitation in real-world scenarios. In our setting, the robot was limited in autonomy with regard to Speaker Identification abilities because the input of the sound source was provided by the experimenter. However, for a final version of the architecture, we are implementing a Sound Localization module to classify the direction of the upcoming sound source with respect to a robot-centric reference frame (e.g., from the right, front, or left of the robot). This will enable the activation of specific attention mechanisms, such as redirecting the robot’s gaze toward the direction of the speakers’ voice when they are outside its field of view.

Another limitation of the XAE deployment in real-time HRI lies in speaker diarization, a critical component for enabling seamless multi-party conversations. In our architecture, audio segmentation relied solely on silence intervals, leading to potential errors when participants spoke simultaneously or paused during their speech. To minimize confusion, participants were informed of these limitations and instructed to avoid speaking simultaneously and to leave sufficient pauses between their utterances, allowing the robot to accurately distinguish and process the speech segments. Moreover, the spatial memory version we employed was limited in granularity, making it insufficient for handling more complex interactions. To address these limitations, we plan to enhance the architecture by integrating a robust speaker diarization model and a more precise spatial memory system. Deploying the model in real-time also presented challenges related to network overload, particularly in maintaining a seamless operation of the modular architecture. As observed in the video, graphical explanations displayed on the TV screen occasionally flickered due to network saturation, which was more frequent during peak usage hours. The modular approach required extensive use of the local network to facilitate information exchange between modules, but this dependency occasionally led to performance bottlenecks. While this design ensures flexibility and scalability, we recognize the potential inconvenience it may cause for users in real-world scenarios and are exploring ways to optimize network usage to mitigate these issues.

Multi-party conversation is a complex challenge that requires robots to solve multiple tasks. We opted for a modular approach to design an architecture scalable to other human-activity recognition skills implemented as additional modules. Multi-modal emotion recognition, Speaker Diarization, Lips Movement Detection, and Voice Recognition are possible skills that can be added to our architecture in the future to increase the robot’s awareness of the social dynamics in multi-party conversation. However, the modularity of our architecture and its deployment via YARP middleware also pose limitations. To be fully scalable, the modular architecture would require adapting the modules that are specifically tailored to the iCub robot (e.g., the iKinGazeCtrl module that controls the robot’s oculomotor behavior and the other modules linked to it).

With respect to scalability, different is the case for the proposed AE models, which can be easily re-used in other robotic platforms, if provided with a visual input, which can be processed into the face and pose data streams. To further enhance the generalization capabilities of our modules, the visual input can be processed using a pre-trained ViT, and fine-tuned on the specific downstream task, even if the physical robot is different (and e.g., is looking at the scene from a different angle). Our architectural design also allows for a broader modality merge, where it is sufficient that we have a ubiquitous representation of each modality. This means that we can merge all sources to create the overall representation and still be able to explain the relative contributions of each input data streams. Moreover, the attention modules used to generate explanations from the XAE model can be utilized in other scenarios as long as there are means to communicate the explanations to the users (i.e., audio output for verbal explanations and a screen for visual explanations).

The online user study was essential to assess how users evaluated the proposed Explainability and Transparency System. It confirmed the importance of leveraging multi-modality for communication in the HRI context but also revealed that the embodied modality needs to be carefully designed. While robots' non-verbal behavior can convey information without interrupting the flow of conversation, it may lead to ambiguous communication, making it less effective in supporting transparency. This was the case, for instance, of our iCub's facial expressions, which participants did not consider as much satisfying and useful as verbal communication. Future work should draw inspiration from this cross-disciplinary study by combining the development of robotic XAI solutions with an assessment of their actual evaluation by users.

6 Conclusion

The development of autonomous robots often aims at their deployment in social environments. Might they be hospitals, schools, restaurants, offices, or homes, robots are required to work safely and efficiently, two things that in human-populated contexts require social-like abilities to perceive the (social) world and act accordingly. To prove their reliability, autonomous systems must be transparent and explainable, two qualities that can increase the users' trust in robots if the former are put in a position to interpret the behavior of the latter.

This work first proposes an explainable machine learning model to solve the problem of addressee estimation, that is, figuring out to whom an interlocutor is speaking within a multi-party conversation. Next, we embedded such a model in a modular architecture to enable the iCub robot to actively participate in such complex interactions. Finally, we proposed a setting in which we assessed the feasibility of the overall architecture while collecting the impressions of users on the robot's explainability and transparency mechanisms.

Thanks to our attention-based approach, our model does not require any additional processing to provide explanations fast, while also increasing the level of transparency. The saliency map of the speaker's face, the relative importance of each input feature, and insights about which parts of the interaction affected the robot's estimate the most are acquired from our model and integrated with other techniques to clarify the opacity of the iCub robot's decision in a challenging scenario such as multi-party conversation.

When it comes to deploying deep neural networks in robots to predict human behavior and engage in social interaction, it is fundamental to adopt a unified approach. From neural network design to the implementation of computer vision algorithms into a modular architecture, ending with an exploratory user study, our work sought to do this by considering and integrating different perspectives to unveil the opacity of artificial systems designed to interact with us.

Acknowledgments

The research leading to these results has received funding from the project titled TERAIS in the framework of the program Horizon-Widera-2021 of the European Union under the Grant agreement number 101079338.

I. Bečková and Š. Pócoš were also supported in part by The Slovak Research and Development Agency, project no. APVV-21-0105.

This Preprint has been prepared based on the following template: <https://github.com/kourgeorge/arxiv-style.git>

References

Addlesee, A., Cherakara, N., Nelson, N., Hernández García, D., Gunson, N., Sieńska, W., Romeo, M., Dondrup, C., and Lemon, O. (2024). A multi-party conversational social robot using llms. In *Companion of the 2024 ACM/IEEE*

- International Conference on Human-Robot Interaction*, HRI '24, page 1273–1275, New York, NY, USA. Association for Computing Machinery.
- Agarwal, C., Tanneru, S. H., and Lakkaraju, H. (2024). Faithfulness vs. plausibility: On the (un)reliability of explanations from large language models.
- Arumugam, B., Bhattacharjee, S. D., and Yuan, J. (2022). Multimodal attentive learning for real-time explainable emotion recognition in conversations. In *2022 IEEE International Symposium on Circuits and Systems (ISCAS)*, pages 1210–1214.
- Atkinson, R. and Shiffrin, R. (1968). Human memory: A proposed system and its control processes. volume 2 of *Psychology of Learning and Motivation*, pages 89–195. Academic Press.
- Auer, P. (2018). *Gaze, addressee selection and turn-taking in three-party interaction*, pages 197–231. John Benjamins Amsterdam.
- Bae, Y.-H. and Bennett, C. C. (2023). Real-time multimodal turn-taking prediction to enhance cooperative dialogue during human-agent interaction. In *2023 32nd IEEE International Conference on Robot and Human Interactive Communication (RO-MAN)*, pages 2037–2044.
- Barredo Arrieta, A., Díaz-Rodríguez, N., Del Ser, J., Bennetot, A., Tabik, S., Barbado, A., Garcia, S., Gil-Lopez, S., Molina, D., Benjamins, R., Chatila, R., and Herrera, F. (2020). Explainable artificial intelligence (xai): Concepts, taxonomies, opportunities and challenges toward responsible ai. *Information Fusion*, 58:82–115.
- Belgiovine, G., Gonzalez-Billandon, J., Sciutti, A., Sandini, G., and Rea, F. (2022). Hri framework for continual learning in face recognition. In *2022 IEEE/RSJ International Conference on Intelligent Robots and Systems (IROS)*, pages 8226–8233. IEEE.
- Bernotat, J., Eyssel, F., and Sachse, J. (2021). The (fe) male robot: how robot body shape impacts first impressions and trust towards robots. *International Journal of Social Robotics*, 13(3):477–489.
- Bewley, A., Ge, Z., Ott, L., Ramos, F., and Upcroft, B. (2016). Simple online and realtime tracking. In *2016 IEEE international conference on image processing (ICIP)*, pages 3464–3468. IEEE.
- Biewald, L. (2020). Experiment tracking with weights and biases. Software available from wandb.com.
- Bilac, M., Chamoux, M., and Lim, A. (2017). Gaze and filled pause detection for smooth human-robot conversations. In *2017 IEEE-RAS 17th International Conference on Humanoid Robotics (Humanoids)*, pages 297–304.
- Brauwiers, G. and Frasincar, F. (2023). A general survey on attention mechanisms in deep learning. *IEEE Transactions on Knowledge and Data Engineering*, 35(4):3279–3298.
- Cao, Z., Hidalgo Martinez, G., Simon, T., Wei, S., and Sheikh, Y. A. (2019). Openpose: Realtime multi-person 2d pose estimation using part affinity fields. *IEEE Transactions on Pattern Analysis and Machine Intelligence*.
- Chakraborti, T., Sreedharan, S., Zhang, Y., and Kambhampati, S. (2017). Plan explanations as model reconciliation: Moving beyond explanation as soliloquy. In *Proceedings of the 26th International Joint Conference on Artificial Intelligence, IJCAI'17*, page 156–163. AAAI Press.
- Cho, K., van Merriënboer, B., Bahdanau, D., and Bengio, Y. (2014). On the properties of neural machine translation: Encoder–decoder approaches. In *Proceedings of SSST-8, Eighth Workshop on Syntax, Semantics and Structure in Statistical Translation*, pages 103–111. Association for Computational Linguistics.
- Ciatto, G., Schumacher, M. I., Omicini, A., and Calvaresi, D. (2020). Agent-based explanations in ai: Towards an abstract framework. In *Explainable, Transparent Autonomous Agents and Multi-Agent Systems*, pages 3–20. Springer International Publishing.
- Conati, C., Barral, O., Putnam, V., and Rieger, L. (2021). Toward personalized xai: A case study in intelligent tutoring systems. *Artificial Intelligence*, 298:103503.
- De Graaf, M. M. and Malle, B. F. (2017). How people explain action (and autonomous intelligent systems should too). In *2017 AAAI Fall Symposium Series*.
- Dhaussy, T., Jabaian, B., Lefèvre, F., and Horaud, R. (2023). Audio-visual speaker diarization in the framework of multi-user human-robot interaction. In *ICASSP 2023 - 2023 IEEE International Conference on Acoustics, Speech and Signal Processing (ICASSP)*, pages 1–5.
- Dosovitskiy, A., Beyler, L., Kolesnikov, A., Weissenborn, D., Zhai, X., Unterthiner, T., Dehghani, M., Minderer, M., Heigold, G., Gelly, S., Uszkoreit, J., and Houlsby, N. (2021). An image is worth 16x16 words: Transformers for image recognition at scale. In *International Conference on Learning Representations*.

- Eldardeer, O., Gonzalez-Billandon, J., Grasse, L., Tata, M., and Rea, F. (2021). A biological inspired cognitive framework for memory-based multi-sensory joint attention in human-robot interactive tasks. *Frontiers in Neurorobotics*, 15.
- Fiske, S. T., Cuddy, A. J., and Glick, P. (2007). Universal dimensions of social cognition: Warmth and competence. *Trends in cognitive sciences*, 11(2):77–83.
- Gallucci, M. (2019). Gamlj: General analyses for linear models. *Jamovi Module*.
- Gallucci, M. (2020). jamm: jamovi advanced mediation models. *jamovi module*.
- Gambino, A. and Liu, B. (2022). Considering the context to build theory in hci, hri, and hmc: Explicating differences in processes of communication and socialization with social technologies. *Human-Machine Communication*, 4:111–130.
- Gilpin, L. H., Bau, D., Yuan, B. Z., Bajwa, A., Specter, M., and Kagal, L. (2018). Explaining explanations: An overview of interpretability of machine learning. In *2018 IEEE 5th International Conference on Data Science and Advanced Analytics (DSAA)*, pages 80–89.
- Gray, H. M., Gray, K., and Wegner, D. M. (2007). Dimensions of mind perception. *Science*, 315(5812):619–619.
- Groß, A., Singh, A., Banh, N. C., Richter, B., Scharlau, I., Rohlfing, K. J., and Wrede, B. (2023). Scaffolding the human partner by contrastive guidance in an explanatory human-robot dialogue. *Frontiers in Robotics and AI*, 10.
- Gu, J.-C., Tao, C., and Ling, Z.-H. (2022). Who says what to whom: A survey of multi-party conversations. In *Proceedings of the Thirty-First International Joint Conference on Artificial Intelligence (IJCAI-22)*.
- Halilovic, A. and Lindner, F. (2023). Visuo-textual explanations of a robot’s navigational choices. In *Companion of the 2023 ACM/IEEE International Conference on Human-Robot Interaction, HRI ’23*, page 531–535, New York, NY, USA. Association for Computing Machinery.
- He, K., Zhang, X., Ren, S., and Sun, J. (2015). Delving deep into rectifiers: Surpassing human-level performance on imagenet classification. In *2015 IEEE International Conference on Computer Vision (ICCV)*, pages 1026–1034.
- Hilton, D. J. (1990). Conversational processes and causal explanation. *Psychological Bulletin*, 107(1):65.
- Hoffman, R. R., Mueller, S. T., Klein, G., and Litman, J. (2018). Metrics for explainable ai: Challenges and prospects. *arXiv preprint arXiv:1812.04608*.
- Huang, H.-H., Baba, N., and Nakano, Y. (2011). Making virtual conversational agent aware of the addressee of users’ utterances in multi-user conversation using nonverbal information. In *Proceedings of the 13th International Conference on Multimodal Interfaces, ICMI ’11*, page 401–408, New York, NY, USA. Association for Computing Machinery.
- Ishii, R., Otsuka, K., Kumano, S., and Yamato, J. (2016). Prediction of who will be the next speaker and when using gaze behavior in multiparty meetings. *ACM Trans. Interact. Intell. Syst.*, 6(1).
- Jakobson, R. (1981). *Linguistics and Poetics*, pages 18–51. De Gruyter Mouton, Berlin, Boston.
- Jayagopi, D. B., Sheikhi, S., Klotz, D., Wienke, J., Odobez, J.-M., Wrede, S., Khalidov, V., Nguyen, L., Wrede, B., and Gatica-Perez, D. (2012). The vernissage corpus: A multimodal human-robot-interaction dataset. Technical report.
- Jayagopi, D. B., Sheiki, S., Klotz, D., Wienke, J., Odobez, J.-M., Wrede, S., Khalidov, V., Nguyen, L., Wrede, B., and Gatica-Perez, D. (2013). The vernissage corpus: A conversational human-robot-interaction dataset. In *2013 8th ACM/IEEE International Conference on Human-Robot Interaction (HRI)*, pages 149–150. IEEE.
- Jiang, A. Q., Sablayrolles, A., Mensch, A., Bamford, C., Chaplot, D. S., de las Casas, D., Bressand, F., Lengyel, G., Lample, G., Saulnier, L., Lavaud, L. R., Lachaux, M.-A., Stock, P., Scao, T. L., Lavril, T., Wang, T., Lacroix, T., and Sayed, W. E. (2023). Mistral 7b.
- Joher, G., Chaurasia, A., and Qiu, J. (2023). Ultralytics yolo.
- Kashefi, R., Berekatayn, L., Sabokrou, M., and Aghaeipoor, F. (2023). Explainability of vision transformers: A comprehensive review and new perspectives. *arXiv preprint arXiv:2311.06786*.
- Kerzel, M., Ambsdorf, J., Becker, D., Lu, W., Strahl, E., Spisak, J., Gäde, C., Weber, T., and Wermter, S. (2022). What’s on your mind, nico? *KI - Künstliche Intelligenz*, 36(3):237–254.
- Kotseruba, I. and Tsotsos, J. K. (2020). 40 years of cognitive architectures: core cognitive abilities and practical applications. *Artificial Intelligence Review*, 53(1):17–94.
- Krizhevsky, A., Sutskever, I., and Hinton, G. E. (2012). Imagenet classification with deep convolutional neural networks. In *Advances in Neural Information Processing Systems*, volume 25. Curran Associates, Inc.
- Lai, V., Chen, C., Liao, Q. V., Smith-Renner, A., and Tan, C. (2021). Towards a science of human-ai decision making: a survey of empirical studies. *arXiv preprint arXiv:2112.11471*.

- Lundberg, S. M. and Lee, S.-I. (2017). A unified approach to interpreting model predictions. In Guyon, I., Luxburg, U. V., Bengio, S., Wallach, H., Fergus, R., Vishwanathan, S., and Garnett, R., editors, *Advances in Neural Information Processing Systems*, volume 30. Curran Associates, Inc.
- Maruyama, Y., Fukui, H., Hirakawa, T., Yamashita, T., Fujiyoshi, H., and Sugiura, K. (2022). Visual explanation of deep q-network for robot navigation by fine-tuning attention branch. *arXiv preprint arXiv:2208.08613*.
- Matarese, M., Cocchella, F., Rea, F., and Sciutti, A. (2023a). Ex(plainable) machina: how social-implicit xai affects complex human-robot teaming tasks. In *2023 IEEE International Conference on Robotics and Automation (ICRA)*, pages 11986–11993.
- Matarese, M., Cocchella, F., Rea, F., and Sciutti, A. (2023b). Natural born explainees: how users’ personality traits shape the human-robot interaction with explainable robots. In *2023 32nd IEEE International Conference on Robot and Human Interactive Communication (RO-MAN)*, pages 1786–1793.
- Matarese, M., Sciutti, A., Rea, F., and Rossi, S. (2021). Toward robots’ behavioral transparency of temporal difference reinforcement learning with a human teacher. *IEEE Transactions on Human-Machine Systems*, 51(6):578–589.
- Mazzola, C., Rea, F., and Sciutti, A. (2024). Real-time addressee estimation: Deployment of a deep-learning model on the icub robot. In *Proceedings of the 2023 I-RIM Conference*.
- Mazzola, C., Romeo, M., Rea, F., Sciutti, A., and Cangelosi, A. (2023). To whom are you talking? a deep learning model to endow social robots with addressee estimation skills. In *2023 International Joint Conference on Neural Networks (IJCNN)*, pages 1–10.
- McInnes, L., Healy, J., Saul, N., and Großberger, L. (2018). UMAP: Uniform manifold approximation and projection. *Journal of Open Source Software*, 3(29):861.
- McMahon, E. and Isik, L. (2023). Seeing social interactions. *Trends in Cognitive Sciences*, 27(12):1165–1179. doi: 10.1016/j.tics.2023.09.001.
- Metta, G., Fitzpatrick, P., and Natale, L. (2006). Yarp: Yet another robot platform. *International Journal of Advanced Robotic Systems*, 3(1):8.
- Miller, T. (2019). Explanation in artificial intelligence: Insights from the social sciences. *Artificial Intelligence*, 267:1–38.
- Niu, Z., Zhong, G., and Yu, H. (2021). A review on the attention mechanism of deep learning. *Neurocomputing*, 452:48–62.
- Osokin, D. (2018). Real-time 2d multi-person pose estimation on cpu: Lightweight openpose. In *arXiv preprint arXiv:1811.12004*.
- Radford, A., Kim, J. W., Xu, T., Brockman, G., Mcleavey, C., and Sutskever, I. (2023). Robust speech recognition via large-scale weak supervision. In Krause, A., Brunskill, E., Cho, K., Engelhardt, B., Sabato, S., and Scarlett, J., editors, *Proceedings of the 40th International Conference on Machine Learning*, volume 202 of *Proceedings of Machine Learning Research*, pages 28492–28518. PMLR.
- Ribeiro, M. T., Singh, S., and Guestrin, C. (2016). Why should i trust you?: Explaining the predictions of any classifier. *Proceedings of the 22nd ACM SIGKDD International Conference on Knowledge Discovery and Data Mining*.
- Richter, V., Carlmeyer, B., Lier, F., Meyer zu Borgsen, S., Schlangen, D., Kummert, F., Wachsmuth, S., and Wrede, B. (2016). Are you talking to me? improving the robustness of dialogue systems in a multi party hri scenario by incorporating gaze direction and lip movement of attendees. In *Proceedings of the Fourth International Conference on Human Agent Interaction, HAI '16*, page 43–50, New York, NY, USA. Association for Computing Machinery.
- Robrecht, A. S. and Kopp, S. (2023). Snape: A sequential non-stationary decision process model for adaptive explanation generation. In *ICAART (1)*, pages 48–58.
- Rohlfing, K. J., Cimiano, P., Scharlau, I., Matzner, T., Buhl, H. M., Buschmeier, H., Esposito, E., Grimminger, A., Hammer, B., Häb-Umbach, R., Horwath, I., Hüllermeier, E., Kern, F., Kopp, S., Thommes, K., Ngonga Ngomo, A.-C., Schulte, C., Wachsmuth, H., Wagner, P., and Wrede, B. (2021). Explanation as a social practice: Toward a conceptual framework for the social design of ai systems. *IEEE Transactions on Cognitive and Developmental Systems*, 13(3):717–728.
- Roncone, A., Pattacini, U., Metta, G., and Natale, L. (2016). A cartesian 6-dof gaze controller for humanoid robots. In *Robotics: science and systems*, volume 2016.
- Saade, P. (2023). Optimizing the portability of an addressee estimation model in the icub social robot. Master’s thesis, University of Genoa.
- Sciutti, A., Mara, M., Tagliasco, V., and Sandini, G. (2018). Humanizing human-robot interaction: On the importance of mutual understanding. *IEEE Technology and Society Magazine*, 37(1):22–29.

- Selkowitz, A. R., Larios, C. A., Lakhmani, S. G., and Chen, J. Y. (2017). Displaying information to support transparency for autonomous platforms. In Savage-Knepshiehl, P. and Chen, J., editors, *Advances in Human Factors in Robots and Unmanned Systems*, pages 161–173, Cham. Springer International Publishing.
- Selvaraju, R. R., Cogswell, M., Das, A., Vedantam, R., Parikh, D., and Batra, D. (2017). Grad-CAM: Visual explanations from deep networks via gradient-based localization. In *IEEE International Conference on Computer Vision*, pages 618–626.
- Setchi, R., Dehkordi, M. B., and Khan, J. S. (2020). Explainable robotics in human-robot interactions. *Procedia Computer Science*, 176:3057–3066. Knowledge-Based and Intelligent Information & Engineering Systems: Proceedings of the 24th International Conference KES2020.
- Sheikhi, S., Babu Jayagopi, D., Khalidov, V., and Odobez, J.-M. (2013). Context aware addressee estimation for human robot interaction. In *GazeIn '13: Proceedings of the 6th workshop on Eye gaze in intelligent human machine interaction: gaze in multimodal interaction*, GazeIn '13, page 1–6, New York, NY, USA. Association for Computing Machinery.
- Shen, T., Zhou, T., Long, G., Jiang, J., Pan, S., and Zhang, C. (2017). Disan: Directional self-attention network for rnn/cnn-free language understanding. *Proceedings of the AAAI Conference on Artificial Intelligence*, 32.
- Simonyan, K., Vedaldi, A., and Zisserman, A. (2014). Deep inside convolutional networks: Visualising image classification models and saliency maps. In *Workshop at International Conference on Learning Representations*.
- Sinha, P., Mitra, P., da Costa, A. A. B., and Kekatos, N. (2021). Explaining outcomes of multi-party dialogues using causal learning. *arXiv preprint arXiv:2105.00944*.
- Skantze, G. (2021). Turn-taking in conversational systems and human-robot interaction: A review. *Computer Speech & Language*, 67:101178.
- Sobrin-Hidalgo, D., González-Santamarta, M. Á., Guerrero-Higueras, Á. M., Rodríguez-Lera, F. J., and Matellán-Olivera, V. (2024). Enhancing robot explanation capabilities through vision-language models: a preliminary study by interpreting visual inputs for improved human-robot interaction. *arXiv preprint arXiv:2404.09705*.
- Spaccatini, F., Pacilli, M. G., Giovannelli, I., Roccatò, M., and Penone, G. (2019). Sexualized victims of stranger harassment and victim blaming: The moderating role of right-wing authoritarianism. *Sexuality & Culture*, 23(3):811–825.
- Stange, S., Hassan, T., Schröder, F., Konkol, J., and Kopp, S. (2022). Self-explaining social robots: An explainable behavior generation architecture for human-robot interaction. *Frontiers in Artificial Intelligence*, page 87.
- Tabrez, A., Agrawal, S., and Hayes, B. (2019). Explanation-based reward coaching to improve human performance via reinforcement learning. In *2019 14th ACM/IEEE International Conference on Human-Robot Interaction (HRI)*, pages 249–257. IEEE.
- Tesema, F. B., Gu, J., Song, W., Wu, H., Zhu, S., Lin, Z., Huang, M., Wang, W., and Kumar, R. (2023). Addressee detection using facial and audio features in mixed human-human and human-robot settings: A deep learning framework. *IEEE Systems, Man, and Cybernetics Magazine*, 9(2):25–38.
- The jamovi project (2023). jamovi. Computer Software.
- Tonmoy, S. M. T. I., Zaman, S. M. M., Jain, V., Rani, A., Rawte, V., Chadha, A., and Das, A. (2024). A comprehensive survey of hallucination mitigation techniques in large language models.
- van der Maaten, L. and Hinton, G. (2008). Visualizing data using t-SNE. *Journal of Machine Learning Research*, 9(86):2579–2605.
- van Turnhout, K., Terken, J., Bakx, I., and Eggen, B. (2005). Identifying the intended addressee in mixed human-human and human-computer interaction from non-verbal features. In *Proceedings of the 7th International Conference on Multimodal Interfaces, ICMI '05*, page 175–182, New York, NY, USA. Association for Computing Machinery.
- Vaswani, A., Shazeer, N., Parmar, N., Uszkoreit, J., Jones, L., Gomez, A. N., Kaiser, L., and Polosukhin, I. (2017). Attention is all you need. In *Advances in Neural Information Processing Systems*, volume 30. Curran Associates, Inc.
- Vernon, D. (2014). *Artificial cognitive systems: A primer*.
- Wightman, R. (2019). Pytorch image models. *GitHub repository*.
- Wortham, R. H., Theodorou, A., and Bryson, J. J. (2016). What does the robot think? transparency as a fundamental design requirement for intelligent systems. In *IJCAI 2016 Ethics for AI Workshop*.
- Wortham, R. H., Theodorou, A., and Bryson, J. J. (2017). Robot transparency: Improving understanding of intelligent behaviour for designers and users. In *Towards Autonomous Robotic Systems: 18th Annual Conference, TAROS 2017, Guildford, UK, July 19–21, 2017, Proceedings. Lecture Notes in Artificial Intelligence*, pages 274–289. Springer.

- Zhou, B., Khosla, A., Lapedriza, A., Oliva, A., and Torralba, A. (2016). Learning deep features for discriminative localization. In *IEEE Conference on Computer Vision and Pattern Recognition (CVPR)*, pages 2921–2929.
- Zhu, H., Yu, C., and Cangelosi, A. (2022). Affective human-robot interaction with multimodal explanations. In *International Conference on Social Robotics*, pages 241–252. Springer.

Appendix A - List of abbreviations

Abbreviations	
AE	Addressee Estimation
HRI	Human-Robot Interaction
IAE	Improved Addressee Estimation (model)
LLM	Large Language Models
MOT	Multi-Object Tracker
SOTA	State of the art
XAE	Explainable Addressee Estimation (model)
XAI	Explainable Artificial Intelligence

Appendix B - Design of the attention-based explainable AE model: Additional methods for merging modalities

To merge the two data streams, we also tested some additional architectural concepts. However, these methods neither significantly surpassed the baseline accuracy nor brought clear explanations to the user.

Modality merge using multi-dimensional attention

In this part, we are going to transform the two modalities of pose and image vector. We base it on the mechanism of multi-dimensional attention proposed in Shen et al. (2017), where the authors propose an attention scoring not only to weight individual value vectors but to give each of their elements a corresponding weight as well. For a given time frame t , using this procedure we are able to merge two modalities (outputs of the face and pose networks, $\mathbf{f}_t \in \mathbb{R}^{d_{\text{face}}}$ and $\mathbf{p}_t \in \mathbb{R}^{d_{\text{pose}}}$ respectively) into a single representation, which is then fed to the final, recurrent network. Using this method, the modalities are combined while taking into account their cross-relations. Our divergence from the traditional approach is that we do not combine multiple value vectors to a single representation, but we rather compute one value vector at a time and feed it to the RNN. The exact computation is following:

$$\mathbf{q}_t = \mathbf{W}^Q \mathbf{p}_t, \quad \mathbf{k}_t = \mathbf{W}^K \mathbf{f}_t, \quad \mathbf{v}_t = \mathbf{W}^V \mathbf{f}_t, \quad (\text{B.1})$$

where the matrices, $\mathbf{W}^Q \in \mathbb{R}^{d_q \times d_{\text{pose}}}$, $\mathbf{W}^K \in \mathbb{R}^{d_k \times d_{\text{face}}}$ and $\mathbf{W}^V \in \mathbb{R}^{d_v \times d_{\text{face}}}$ are trainable parameters representing transformation of the corresponding vectors to query, key and value.

The next step is to compute the importance weights for each of the elements of the value vector.

$$\mathbf{e}_t = \mathbf{W}_D^T \times \text{act}(\mathbf{W}_1 \times \mathbf{q}_t + \mathbf{W}_2 \times \mathbf{k}_t + \mathbf{b}), \quad (\text{B.2})$$

where $\mathbf{W}_1 \in \mathbb{R}^{d_{\text{inner}} \times d_q}$, $\mathbf{W}_2 \in \mathbb{R}^{d_{\text{inner}} \times d_k}$, $\mathbf{W}_D \in \mathbb{R}^{d_{\text{inner}} \times d_v}$ and $\mathbf{b} \in \mathbb{R}^{d_{\text{inner}}}$ are trainable parameters.

The input to the RNN network is a simple Hadamard product of \mathbf{e}_t and \mathbf{v}_t . Thus, each element of the value vector has its corresponding weight.

Modality merge using general attention

In this method we leverage the idea of general attention procedure (Brauwers and Frasinca, 2023). After the input is processed, we end up with a representation of pose and face, \mathbf{p}_t and \mathbf{f}_t , respectively. However in this scenario, $\mathbf{f}_t \in \mathbb{R}^{d_{\text{pose}}}$ is a vector but $\mathbf{p}_t \in \mathbb{R}^{n_p \times d_{\text{embed}}}$ is a series of vectors, each corresponding to a channel aggregation for a single pixel value after the convolutions.

To continue with a general scheme of attention, we create our query, keys, and values as follows:

$$\mathbf{q}_t = \mathbf{W}^Q \mathbf{p}_t, \quad \mathbf{k}_{t,i} = \mathbf{W}^K \mathbf{f}_{t,i}, \quad \mathbf{v}_{t,i} = \mathbf{W}^V \mathbf{f}_{t,i}, \quad (\text{B.3})$$

where the matrices, $\mathbf{W}^Q \in \mathbb{R}^{d_q \times d_{\text{pose}}}$, $\mathbf{W}^K \in \mathbb{R}^{d_k \times d_{\text{face}}}$ and $\mathbf{W}^V \in \mathbb{R}^{d_v \times d_{\text{face}}}$ are trainable parameters representing transformation of the corresponding vectors to query, key and value. A scoring function is applied to return the corresponding weight to each of the components of the face representation:

$$\mathbf{e}_{t,i} = \mathbf{w}_D^T \times \text{act}(\mathbf{W}_1 \times \mathbf{q}_t + \mathbf{W}_2 \times \mathbf{k}_{t,i} + \mathbf{b}), \quad (\text{B.4})$$

where $\mathbf{W}_1 \in \mathbb{R}^{d_{\text{inner}} \times d_q}$, $\mathbf{W}_2 \in \mathbb{R}^{d_{\text{inner}} \times d_k}$, $\mathbf{W}_D \in \mathbb{R}^{d_{\text{inner}}}$ and $\mathbf{b} \in \mathbb{R}^{d_{\text{inner}}}$ are trainable parameters. This is followed by an alignment step, where we normalize the contribution of each component of the face representation.

$$a_{t,i} = \text{softmax}(e_{t,i}; \mathbf{e}). \quad (\text{B.5})$$

The final representation \mathbf{r} of the input is a weighted sum of the face components.

$$\mathbf{r}_t = \sum_{i=1}^{n_p} a_{t,i} \cdot \mathbf{v}_{t,i}. \quad (\text{B.6})$$

Appendix C - Deployment of the XAE in a modular architecture: Prompts for the LLM agent

Shopping Mall Context:

“You are a service robot named iCub, working as an assistant in shopping mall. You help customers who need information about shops inside the mall. You give informations based on customers needs and preferences. Be friendly and keep answers very short and concise!”

Domestic Assistant Context:

“You are a domestic assistant robot named iCub. You can do several tasks, like preparing drinks and food, and your role is to help accomplish this task when required. Be friendly and keep answers very short and concise!”

Restaurant Context:

“You are a service robot named iCub, working as a waiter for a restaurant. You help customers who need to order their food and drinks. Be friendly and keep answers very short and concise!”

LLM-based AE Predictions Context:

“You are a robot taking part in a conversation with one or more people. Given who is speaking (the Speaker) and what the speaker says (the Message), identify who is the sentence’s addressee. Choose among only two options: [Myself, the ROBOT], [Another person, NOT THE ROBOT]. Answer in the format: Addressee: [option].”

Appendix D - Online User Study: Additional Analysis

Analysis of relationships between the three explanation evaluation criteria via correlation matrices

Table D.1: Correlation matrix in the verbal modality.

Correlation Matrix		Satisfaction	Usefulness	Intrusiveness
Satisfaction	Spearman’s ρ	—		
	df	—		
	p-value	—		
Usefulness	Spearman’s ρ	.512	***	—
	df	58	—	
	p-value	<.001	—	
Intrusiveness	Spearman’s ρ	-.293	*	-.221
	df	58	58	—
	p-value	.023	.089	—

Note. * $p < .05$, ** $p < .01$, *** $p < .001$

Table D.2: Correlation matrix in the embodied modality.
Correlation Matrix

		Satisfaction	Usefulness	Intrusiveness
Satisfaction	Spearman's ρ	—		
	df	—		
	p-value	—		
Usefulness	Spearman's ρ	.770 ***	—	
	df	58	—	
	p-value	<.001	—	
Intrusiveness	Spearman's ρ	-.285 *	-.262 *	—
	df	58	58	—
	p-value	.027	.043	—

Note. * $p < .05$, ** $p < .01$, *** $p < .001$

Table D.3: Correlation matrix in the graphical modality.
Correlation Matrix

		Satisfaction	Usefulness	Intrusiveness
Satisfaction	Spearman's ρ	—		
	df	—		
	p-value	—		
Usefulness	Spearman's ρ	.711 ***	—	
	df	58	—	
	p-value	<.001	—	
Intrusiveness	Spearman's ρ	-.473 ***	-.376 **	—
	df	58	58	—
	p-value	<.001	.003	—

Note. * $p < .05$, ** $p < .01$, *** $p < .001$

Gender effect on evaluation of explanation modalities

Tables D.4 and D.5 report the results of post-hoc tests from Mixed Model analysis on participants' evaluations of explanation modalities in terms of Satisfaction D.4 and Usefulness D.5. While these models are structured as described in Section 4.4 (§Questionnaires and Analysis), we now included Gender as an additional factor. Therefore, Satisfaction, Usefulness, and Intrusiveness were used as dependent variables, while Modality and Gender were included as factors. The Intrusiveness model did not reveal any statistically significant results in post-hoc tests. Conversely, significant differences were found in the Satisfaction models when comparing both verbal and graphical modalities to embodied, and in the Usefulness model when comparing verbal to embodied. These differences were significant only within the female group; however, the main effect of Gender was not statistically significant in post-hoc tests across the three scales (Satisfaction M.-F.: $B = -.07$, $t(58) = -.21$, $p = .83$; Usefulness M.-F.: $B = .621$, $t(58) = 1.47$, $p = .15$; Intrusiveness M.-F.: $B = -.06$, $t(58) = -.13$, $p = .89$). In conclusion, it remains unclear whether the modality differences observed only in the female group (in line with previous findings, see Section 4.2) can be explained as a Gender effect or are instead due to the larger female sample size, potentially leading to limited statistical power for the male subgroup analysis. Future studies could further explore this potential impact as well as investigate whether participants' educational background (technical vs. non-technical) may also play a role.

Insights on XAI user evaluation for each modality

To understand how much explanations provided by the robot about its functioning contributed to increasing participants' trust in the robot, we inspected the relationship between the Usefulness of explanations and the two components of Trust (affective and cognitive) and assessed whether participants' perception of the robot's qualities played any role as a mediation factor. In particular, since we designed the robot's explanations to be provided via three different modalities (verbal, embodied and graphical) we verified whether the modalities moderated the abovementioned relationship. The following Tables report the results from the two Conditional Mediation tests designed to assess the abovementioned relationship. Affective and Cognitive Trust were, respectively, the two dependent variables, while Explanation Usefulness played the role of covariate, the five robot's qualities (Experience, Agency, Likeability, Competence and Warmth) were the mediators, and the explanation modality was the moderator.

Table D.4: Results from the post-hoc tests of the Mixed Model Analysis of Modality and Gender effects on Satisfaction
Post Hoc Comparisons - Modality (Mod.) * Gender (Gend.)

Mod.	Gend.	Mod.	Gend.	Diff.	SE	t	df	p
Graph.	M.	Graph.	F.	-.19	0.38	-.49	111	1.00
Graph.	M.	Non-v.	F.	.65	0.38	1.69	111	1.00
Graph.	M.	Verbal	F.	-.44	0.38	-1.16	111	1.00
Non-v.	F.	Graph.	F.	-.83	0.18	-4.64	116	<.001
Non-v.	M.	Graph.	F.	-.58	0.38	-1.51	111	1.00
Non-v.	M.	Graph.	M.	-.39	0.33	-1.20	116	1.00
Non-v.	M.	Non-v.	F.	.25	0.38	0.66	111	1.00
Non-v.	M.	Verbal	F.	-.84	0.38	-2.18	111	.471
Verbal	F.	Graph.	F.	.26	0.18	1.44	116	1.00
Verbal	F.	Non-v.	F.	1.09	0.18	6.08	116	<.001
Verbal	M.	Graph.	F.	-.01	0.38	-0.04	111	1.00
Verbal	M.	Graph.	M.	.17	0.33	.53	116	1.00
Verbal	M.	Non-v.	F.	.82	0.38	2.13	111	.525
Verbal	M.	Non-v.	M.	.56	0.33	1.73	116	1.00
Verbal	M.	Verbal	F.	-.27	0.38	-.71	111	1.00

Table D.5: Results from the post-hoc tests of the Mixed Model Analysis of Modality and Gender effects on Usefulness
Post Hoc Comparisons - Modality (Mod.) * Gender (Gend.)

Mod.	Gend.	Mod.	Gend.	Diff.	SE	t	df	p
Graph.	M.	Graph.	F.	.74	.47	1.58	87.9	1.00
Graph.	M.	Non-v.	F.	1.08	.47	2.3	87.9	.36
Graph.	M.	Verbal	F.	.37	.47	.78	87.9	1.00
Non-v.	F.	Graph.	F.	-.034	.18	-1.93	116	.85
Non-v.	M.	Graph.	F.	.34	.47	.72	87.9	1.00
Non-v.	M.	Graph.	M.	-.04	.32	-1.26	116	1.00
Non-v.	M.	Non-v.	F.	.68	.47	1.44	87.9	1.00
Non-v.	M.	Verbal	F.	-.04	.47	-.08	87.9	.471
Verbal	F.	Graph.	F.	.38	.18	2.13	116	.524
Verbal	F.	Non-v.	F.	.72	.18	4.06	116	.001
Verbal	M.	Graph.	F.	.82	.47	1.73	87.9	1.00
Verbal	M.	Graph.	M.	.07	.32	.23	116	1.00
Verbal	M.	Non-v.	F.	1.16	.47	2.45	87.9	.244
Verbal	M.	Non-v.	M.	.48	.32	1.49	116	1.00
Verbal	M.	Verbal	F.	.44	.47	.93	87.9	1.00

Table D.6: Results from Mediation Model: Usefulness effect on Affective Trust, mediated by robot's characteristics dimensions and moderated by XAI modality.

Conditional Mediation			95% C.I. (a)						
Moderator levels			Estimate	SE	Lower	Upper	β	z	p
Modality	Type	Effect							
Average	Indirect	<i>Usefulness</i> \Rightarrow <i>Experience</i> \Rightarrow <i>AffectiveTrust</i>	-.02	.01	-.04	.01	-.02	-1.43	.15
Average		<i>Usefulness</i> \Rightarrow <i>Agency</i> \Rightarrow <i>AffectiveTrust</i>	.07	.03	.01	.12	.09	2.42	.02
Average		<i>Usefulness</i> \Rightarrow <i>Likeability</i> \Rightarrow <i>AffectiveTrust</i>	.03	.02	-.02	.08	.04	1.25	.21
Average		<i>Usefulness</i> \Rightarrow <i>Competence</i> \Rightarrow <i>AffectiveTrust</i>	.15	.04	.07	.24	.21	3.66	<.001
Average		<i>Usefulness</i> \Rightarrow <i>Warmth</i> \Rightarrow <i>AffectiveTrust</i>	.09	.04	.01	.16	.12	2.28	.02
Average	Component	<i>Usefulness</i> \Rightarrow <i>Experience</i>	.19	.05	.08	.29	.26	3.42	<.001
Average		<i>Experience</i> \Rightarrow <i>AffectiveTrust</i>	-.09	.06	-.21	.02	-.09	-1.58	.11
Average		<i>Usefulness</i> \Rightarrow <i>Agency</i>	.49	.07	.36	.62	.51	7.23	<.001
Average		<i>Agency</i> \Rightarrow <i>AffectiveTrust</i>	.14	.05	.03	.24	.19	2.57	.01
Average		<i>Usefulness</i> \Rightarrow <i>Likeability</i>	.38	.06	.26	.49	.46	6.47	<.001
Average		<i>Likeability</i> \Rightarrow <i>AffectiveTrust</i>	.08	.06	-.04	.2	.09	1.27	.2
Average		<i>Usefulness</i> \Rightarrow <i>Competence</i>	.48	.05	.38	.58	.61	9.45	<.001
Average		<i>Competence</i> \Rightarrow <i>AffectiveTrust</i>	.32	.08	.16	.48	.35	3.97	<.001
Average		<i>Usefulness</i> \Rightarrow <i>Warmth</i>	.61	.06	.48	.73	.61	9.33	<.001
Average		<i>Warmth</i> \Rightarrow <i>AffectiveTrust</i>	.14	.06	.02	.26	.2	2.35	.02
Average	Direct	<i>Usefulness</i> \Rightarrow <i>AffectiveTrust</i>	.1	.05	.01	.19	.14	2.18	.03
Average	Total	<i>Usefulness</i> \Rightarrow <i>AffectiveTrust</i>	.42	.05	.33	.51	.59	8.87	<.001
Verbal	Indirect	<i>Usefulness</i> \Rightarrow <i>Experience</i> \Rightarrow <i>AffectiveTrust</i>	-.01	.01	-.04	.01	-.02	-.94	.35
Verbal		<i>Usefulness</i> \Rightarrow <i>Agency</i> \Rightarrow <i>AffectiveTrust</i>	.09	.04	.01	.17	.12	2.22	.03
Verbal		<i>Usefulness</i> \Rightarrow <i>Likeability</i> \Rightarrow <i>AffectiveTrust</i>	.03	.03	-.03	.1	.05	1.13	.26
Verbal		<i>Usefulness</i> \Rightarrow <i>Competence</i> \Rightarrow <i>AffectiveTrust</i>	.24	.07	.11	.36	.32	3.6	<.001
Verbal		<i>Usefulness</i> \Rightarrow <i>Warmth</i> \Rightarrow <i>AffectiveTrust</i>	.13	.05	.03	.23	.17	2.47	.01
Verbal	Component	<i>Usefulness</i> \Rightarrow <i>Experience</i>	.18	.12	-.05	.4	.25	1.53	.13
Verbal		<i>Experience</i> \Rightarrow <i>AffectiveTrust</i>	-.07	.06	-.19	.05	-.07	-1.19	.24
Verbal		<i>Usefulness</i> \Rightarrow <i>Agency</i>	.65	.14	.37	.93	.67	4.53	<.001
Verbal		<i>Agency</i> \Rightarrow <i>AffectiveTrust</i>	.14	.05	.03	.24	.18	2.54	.01
Verbal		<i>Usefulness</i> \Rightarrow <i>Likeability</i>	.48	.12	.24	.72	.59	3.92	<.001
Verbal		<i>Likeability</i> \Rightarrow <i>AffectiveTrust</i>	.07	.06	-.05	.19	.08	1.18	.24
Verbal		<i>Usefulness</i> \Rightarrow <i>Competence</i>	.66	.11	.45	.87	.85	6.17	<.001
Verbal		<i>Competence</i> \Rightarrow <i>AffectiveTrust</i>	.36	.08	.2	.52	.38	4.43	<.001
Verbal		<i>Usefulness</i> \Rightarrow <i>Warmth</i>	.78	.14	.51	1.04	.78	5.67	<.001
Verbal		<i>Warmth</i> \Rightarrow <i>AffectiveTrust</i>	.17	.06	.05	.29	.22	2.74	.006
Verbal	Direct	<i>Usefulness</i> \Rightarrow <i>AffectiveTrust</i>	.02	.08	-.14	.19	.03	-.29	.77
Verbal	Total	<i>Usefulness</i> \Rightarrow <i>AffectiveTrust</i>	.5	.1	.3	.7	.69	4.98	<.001
Embodied	Indirect	<i>Usefulness</i> \Rightarrow <i>Experience</i> \Rightarrow <i>AffectiveTrust</i>	-.03	.02	-.07	.00	-.04	-1.71	.09
Embodied		<i>Usefulness</i> \Rightarrow <i>Agency</i> \Rightarrow <i>AffectiveTrust</i>	.06	.03	.01	.12	.09	2.22	.03
Embodied		<i>Usefulness</i> \Rightarrow <i>Likeability</i> \Rightarrow <i>AffectiveTrust</i>	.03	.02	-.01	.07	.04	1.38	.17
Embodied		<i>Usefulness</i> \Rightarrow <i>Competence</i> \Rightarrow <i>AffectiveTrust</i>	.12	.04	.04	.2	.17	2.92	.003
Embodied		<i>Usefulness</i> \Rightarrow <i>Warmth</i> \Rightarrow <i>AffectiveTrust</i>	.07	.04	.00	.14	.1	2.05	.04
Embodied	Component	<i>Usefulness</i> \Rightarrow <i>Experience</i>	.24	.08	.07	.4	.34	2.84	.004
Embodied		<i>Experience</i> \Rightarrow <i>AffectiveTrust</i>	-.13	.06	-.24	-.01	-.13	-2.14	.03
Embodied		<i>Usefulness</i> \Rightarrow <i>Agency</i>	.45	.1	.25	.66	.47	4.33	<.001
Embodied		<i>Agency</i> \Rightarrow <i>AffectiveTrust</i>	.14	.05	.03	.24	.19	2.58	.01
Embodied		<i>Usefulness</i> \Rightarrow <i>Likeability</i>	.33	.09	.16	.51	.41	3.69	<.001
Embodied		<i>Likeability</i> \Rightarrow <i>AffectiveTrust</i>	.09	.06	-.03	.21	.1	1.49	.14
Embodied		<i>Usefulness</i> \Rightarrow <i>Competence</i>	.41	.08	.26	.57	.53	5.31	<.001
Embodied		<i>Competence</i> \Rightarrow <i>AffectiveTrust</i>	.28	.08	.12	.44	.31	3.5	<.001
Embodied		<i>Usefulness</i> \Rightarrow <i>Warmth</i>	.55	.1	.35	.74	.55	5.45	<.001
Embodied		<i>Warmth</i> \Rightarrow <i>AffectiveTrust</i>	.13	.06	.02	.25	.19	2.21	.03
Embodied	Direct	<i>Usefulness</i> \Rightarrow <i>AffectiveTrust</i>	.15	.06	.03	.26	.21	2.46	.01
Embodied	Total	<i>Usefulness</i> \Rightarrow <i>AffectiveTrust</i>	.4	.07	.26	.54	.56	5.45	<.001
Graphical	Indirect	<i>Usefulness</i> \Rightarrow <i>Experience</i> \Rightarrow <i>AffectiveTrust</i>	-.01	.01	-.03	.01	-.02	-1.11	.27
Graphical		<i>Usefulness</i> \Rightarrow <i>Agency</i> \Rightarrow <i>AffectiveTrust</i>	.05	.02	.00	.1	.07	2.12	.03
Graphical		<i>Usefulness</i> \Rightarrow <i>Likeability</i> \Rightarrow <i>AffectiveTrust</i>	.02	.02	-.02	.06	.03	1.1	.27
Graphical		<i>Usefulness</i> \Rightarrow <i>Competence</i> \Rightarrow <i>AffectiveTrust</i>	.12	.04	.04	.19	.16	3.07	.002
Graphical		<i>Usefulness</i> \Rightarrow <i>Warmth</i> \Rightarrow <i>AffectiveTrust</i>	.06	.03	.00	.13	.09	1.93	.05
Graphical	Component	<i>Usefulness</i> \Rightarrow <i>Experience</i>	.14	.08	-.01	.3	.2	1.79	.07
Graphical		<i>Experience</i> \Rightarrow <i>AffectiveTrust</i>	-.08	.06	-.2	.03	-.08	-1.41	.16
Graphical		<i>Usefulness</i> \Rightarrow <i>Agency</i>	.37	.1	.17	.57	.38	3.7	<.001
Graphical		<i>Agency</i> \Rightarrow <i>AffectiveTrust</i>	.14	.05	.03	.24	.19	2.58	.01
Graphical		<i>Usefulness</i> \Rightarrow <i>Likeability</i>	.32	.09	.15	.49	.39	3.69	<.001
Graphical		<i>Likeability</i> \Rightarrow <i>AffectiveTrust</i>	.07	.06	-.05	.19	.08	1.15	.25
Graphical		<i>Usefulness</i> \Rightarrow <i>Competence</i>	.36	.07	.22	.51	.46	4.85	<.001
Graphical		<i>Competence</i> \Rightarrow <i>AffectiveTrust</i>	.32	.08	.16	.48	.35	3.97	<.001
Graphical		<i>Usefulness</i> \Rightarrow <i>Warmth</i>	.5	.1	.31	.68	.5	5.18	<.001
Graphical		<i>Warmth</i> \Rightarrow <i>AffectiveTrust</i>	.13	.06	.01	.25	.18	2.09	.04
Graphical	Direct	<i>Usefulness</i> \Rightarrow <i>AffectiveTrust</i>	.13	.06	.02	.23	.18	2.25	.03
Graphical	Total	<i>Usefulness</i> \Rightarrow <i>AffectiveTrust</i>	.37	.07	.23	.5	.51	5.22	<.001

Note 1. Confidence intervals computed with method: Standard (Delta method). Note 2. Betas are completely standardized effect sizes

Table D.7: Results from Mediation Model: Usefulness effect on Cognitive Trust, mediated by robot's characteristics dimensions and moderated by XAI modality.

Conditional Mediation			95% C.I. (a)						
Moderator levels			Estimate	SE	Lower	Upper	β	z	p
Modality	Type	Effect							
Average	Indirect	<i>Usefulness</i> \Rightarrow <i>Experience</i> \Rightarrow <i>CognitiveTrust</i>	-.02	.01	-.04	.01	-.03	-1.33	.19
Average		<i>Usefulness</i> \Rightarrow <i>Agency</i> \Rightarrow <i>CognitiveTrust</i>	.	.03	-.06	.05	-.01	-.19	.85
Average		<i>Usefulness</i> \Rightarrow <i>Likeability</i> \Rightarrow <i>CognitiveTrust</i>	.01	.02	-.04	.05	.01	.32	.75
Average		<i>Usefulness</i> \Rightarrow <i>Competence</i> \Rightarrow <i>CognitiveTrust</i>	.03	.04	-.05	.1	.05	.75	.45
Average		<i>Usefulness</i> \Rightarrow <i>Warmth</i> \Rightarrow <i>CognitiveTrust</i>	.1	.04	.03	.17	.18	2.64	.008
Average	Component	<i>Usefulness</i> \Rightarrow <i>Experience</i>	.19	.05	.08	.29	.26	3.42	<.001
Average		<i>Experience</i> \Rightarrow <i>CognitiveTrust</i>	-.08	.06	-.2	.03	-.11	-1.44	.15
Average		<i>Usefulness</i> \Rightarrow <i>Agency</i>	.49	.07	.36	.62	.51	7.23	<.001
Average		<i>Agency</i> \Rightarrow <i>CognitiveTrust</i>	-.01	.05	-.11	.09	-.02	-.19	.85
Average		<i>Usefulness</i> \Rightarrow <i>Likeability</i>	.38	.06	.26	.49	.46	6.47	<.001
Average		<i>Likeability</i> \Rightarrow <i>CognitiveTrust</i>	.02	.06	-.1	.14	.03	.32	.75
Average		<i>Usefulness</i> \Rightarrow <i>Competence</i>	.48	.05	.38	.58	.61	9.45	<.001
Average		<i>Competence</i> \Rightarrow <i>CognitiveTrust</i>	.06	.08	-.1	.21	.08	.75	.45
Average		<i>Usefulness</i> \Rightarrow <i>Warmth</i>	.61	.06	.48	.73	.61	9.33	<.001
Average		<i>Warmth</i> \Rightarrow <i>CognitiveTrust</i>	.16	.06	.05	.28	.3	2.75	.006
Average	Direct	<i>Usefulness</i> \Rightarrow <i>CognitiveTrust</i>	.2	.04	.11	.28	.36	4.48	<.001
Average	Total	<i>Usefulness</i> \Rightarrow <i>CognitiveTrust</i>	.31	.04	.24	.38	.57	8.5	<.001
Verbal	Indirect	<i>Usefulness</i> \Rightarrow <i>Experience</i> \Rightarrow <i>CognitiveTrust</i>	-.01	.01	-.04	.01	-.02	-.88	.38
Verbal		<i>Usefulness</i> \Rightarrow <i>Agency</i> \Rightarrow <i>CognitiveTrust</i>	-.01	.03	-.08	.06	-.02	-.31	.76
Verbal		<i>Usefulness</i> \Rightarrow <i>Likeability</i> \Rightarrow <i>CognitiveTrust</i>	.01	.03	-.05	.07	.02	.35	.73
Verbal		<i>Usefulness</i> \Rightarrow <i>Competence</i> \Rightarrow <i>CognitiveTrust</i>	.03	.05	-.07	.13	.06	.61	.55
Verbal		<i>Usefulness</i> \Rightarrow <i>Warmth</i> \Rightarrow <i>CognitiveTrust</i>	.13	.05	.03	.23	.25	2.59	.01
Verbal	Component	<i>Usefulness</i> \Rightarrow <i>Experience</i>	.18	.12	-.05	.4	.25	1.53	.13
Verbal		<i>Experience</i> \Rightarrow <i>CognitiveTrust</i>	-.06	.06	-.18	.05	-.08	-1.08	.28
Verbal		<i>Usefulness</i> \Rightarrow <i>Agency</i>	.65	.14	.37	.93	.67	4.53	<.001
Verbal		<i>Agency</i> \Rightarrow <i>CognitiveTrust</i>	-.02	.05	-.12	.09	-.03	-.31	.76
Verbal		<i>Usefulness</i> \Rightarrow <i>Likeability</i>	.48	.12	.24	.72	.59	3.92	<.001
Verbal		<i>Likeability</i> \Rightarrow <i>CognitiveTrust</i>	.02	.06	-.1	.14	.03	.35	.73
Verbal		<i>Usefulness</i> \Rightarrow <i>Competence</i>	.66	.11	.45	.87	.85	6.17	<.001
Verbal		<i>Competence</i> \Rightarrow <i>CognitiveTrust</i>	.05	.08	-.11	.2	.07	.61	.54
Verbal		<i>Usefulness</i> \Rightarrow <i>Warmth</i>	.78	.14	.51	1.04	.78	5.67	<.001
Verbal		<i>Warmth</i> \Rightarrow <i>CognitiveTrust</i>	.17	.06	.06	.29	.32	2.91	.004
Verbal	Direct	<i>Usefulness</i> \Rightarrow <i>CognitiveTrust</i>	.22	.08	.07	.38	.41	2.79	.005
Verbal	Total	<i>Usefulness</i> \Rightarrow <i>CognitiveTrust</i>	.38	.08	.23	.53	.69	4.91	<.001
Embodied	Indirect	<i>Usefulness</i> \Rightarrow <i>Experience</i> \Rightarrow <i>CognitiveTrust</i>	-.03	.02	-.06	.01	-.05	-1.63	.1
Embodied		<i>Usefulness</i> \Rightarrow <i>Agency</i> \Rightarrow <i>CognitiveTrust</i>	.	.02	-.05	.04	-.01	-.13	.89
Embodied		<i>Usefulness</i> \Rightarrow <i>Likeability</i> \Rightarrow <i>CognitiveTrust</i>	.01	.02	-.03	.05	.02	.51	.61
Embodied		<i>Usefulness</i> \Rightarrow <i>Competence</i> \Rightarrow <i>CognitiveTrust</i>	.02	.03	-.04	.09	.04	.67	.51
Embodied		<i>Usefulness</i> \Rightarrow <i>Warmth</i> \Rightarrow <i>CognitiveTrust</i>	.09	.04	.02	.17	.17	2.57	.01
Embodied	Component	<i>Usefulness</i> \Rightarrow <i>Experience</i>	.24	.08	.07	.4	.34	2.84	.004
Embodied		<i>Experience</i> \Rightarrow <i>CognitiveTrust</i>	-.12	.06	-.23	.	-.15	-.2	.05
Embodied		<i>Usefulness</i> \Rightarrow <i>Agency</i>	.45	.1	.25	.66	.47	4.33	<.001
Embodied		<i>Agency</i> \Rightarrow <i>CognitiveTrust</i>	-.01	.05	-.11	.1	-.01	-.13	.89
Embodied		<i>Usefulness</i> \Rightarrow <i>Likeability</i>	.33	.09	.16	.51	.41	3.69	<.001
Embodied		<i>Likeability</i> \Rightarrow <i>CognitiveTrust</i>	.03	.06	-.09	.15	.05	.52	.61
Embodied		<i>Usefulness</i> \Rightarrow <i>Competence</i>	.41	.08	.26	.57	.53	5.31	<.001
Embodied		<i>Competence</i> \Rightarrow <i>CognitiveTrust</i>	.05	.08	-.1	.21	.07	.67	.5
Embodied		<i>Usefulness</i> \Rightarrow <i>Warmth</i>	.55	.1	.35	.74	.55	5.45	<.001
Embodied		<i>Warmth</i> \Rightarrow <i>CognitiveTrust</i>	.17	.06	.06	.29	.31	2.91	.004
Embodied	Direct	<i>Usefulness</i> \Rightarrow <i>CognitiveTrust</i>	.17	.06	.06	.29	.31	2.94	.003
Embodied	Total	<i>Usefulness</i> \Rightarrow <i>CognitiveTrust</i>	.27	.06	.16	.38	.49	4.73	<.001
Graphical	Indirect	<i>Usefulness</i> \Rightarrow <i>Experience</i> \Rightarrow <i>CognitiveTrust</i>	-.01	.01	-.03	.01	-.02	-1.02	.31
Graphical		<i>Usefulness</i> \Rightarrow <i>Agency</i> \Rightarrow <i>CognitiveTrust</i>	.	.02	-.04	.04	.	-.13	.9
Graphical		<i>Usefulness</i> \Rightarrow <i>Likeability</i> \Rightarrow <i>CognitiveTrust</i>	.	.02	-.04	.04	.	.1	.92
Graphical		<i>Usefulness</i> \Rightarrow <i>Competence</i> \Rightarrow <i>CognitiveTrust</i>	.03	.03	-.03	.08	.05	.95	.34
Graphical		<i>Usefulness</i> \Rightarrow <i>Warmth</i> \Rightarrow <i>CognitiveTrust</i>	.07	.03	.01	.13	.13	2.21	.03
Graphical	Component	<i>Usefulness</i> \Rightarrow <i>Experience</i>	.14	.08	-.01	.3	.2	1.79	.07
Graphical		<i>Experience</i> \Rightarrow <i>CognitiveTrust</i>	-.07	.06	-.19	.04	-.09	-1.24	.22
Graphical		<i>Usefulness</i> \Rightarrow <i>Agency</i>	.37	.1	.17	.57	.38	3.7	<.001
Graphical		<i>Agency</i> \Rightarrow <i>CognitiveTrust</i>	-.01	.05	-.11	.1	-.01	-.13	.89
Graphical		<i>Usefulness</i> \Rightarrow <i>Likeability</i>	.32	.09	.15	.49	.39	3.69	<.001
Graphical		<i>Likeability</i> \Rightarrow <i>CognitiveTrust</i>	.01	.06	-.11	.12	.01	.1	.92
Graphical		<i>Usefulness</i> \Rightarrow <i>Competence</i>	.36	.07	.22	.51	.46	4.85	<.001
Graphical		<i>Competence</i> \Rightarrow <i>CognitiveTrust</i>	.08	.08	-.08	.23	.11	.97	.33
Graphical		<i>Usefulness</i> \Rightarrow <i>Warmth</i>	.49	.1	.31	.68	.5	5.18	<.001
Graphical		<i>Warmth</i> \Rightarrow <i>CognitiveTrust</i>	.14	.06	.03	.26	.27	2.44	.02
Graphical	Direct	<i>Usefulness</i> \Rightarrow <i>CognitiveTrust</i>	.2	.05	.09	.31	.37	3.66	<.001
Graphical	Total	<i>Usefulness</i> \Rightarrow <i>CognitiveTrust</i>	.29	.05	.18	.39	.53	5.35	<.001

Note 1. Confidence intervals computed with method: Standard (Delta method). Note 2. Betas are completely standardized effect sizes